NASA Contractor Report

Acousto-Ultrasonic Nondestructive Evaluation of Materials Using Laser Beam Generation and Detection

Robert D. Huber and Robert E. Green, Jr.

Grant NAG3-728

June 1990

NASA

NASA Contractor Report

Acousto-Ultrasonic Nondestructive Evaluation of Materials Using Laser Beam Generation and Detection

Robert D. Huber and Robert E. Green, Jr.
Center for Nondestructive Evaluation
The Johns Hopkins University
Baltimore, MD 21218

Prepared for
Lewis Research Center
under Grant NAG3-728

NASA

National Aeronautics
and Space Administration

Scientific and Technical
Information Division

1990

ABSTRACT

The acousto-ultrasonic method has proven to be a most interesting technique for nondestructive evaluation of the mechanical properties of a variety of materials. Use of the technique, or a modification thereof, has led to correlation of the associated Stress Wave Factor with mechanical properties of both metals and composite materials. This research project applied the method to the nondestructive evaluation of selected fiber reinforced structural composites. In this project, for the first time, conventional piezoelectric transducers were replaced with laser beam ultrasonic generators and detectors. This modification permitted true non-contact acousto-ultrasonic measurements to be made, which yielded new information about the basic mechanisms involved as well as proved the feasibility of making such non-contact measurements on terrestrial and space structures and heat engine components. A state-of-the-art laser based acousto-ultrasonic system, incorporating a compact pulsed laser and a fiber-optic heterodyne interferometer, was delivered to the NASA Lewis Research Center along with this final report.

This report is based on the essay of Mr. Robert D. Huber submitted to The Johns Hopkins University in conformance with the requirements for the degree of Master of Science in Engineering in the Department of Materials Science and Engineering.

TABLE OF CONTENTS

	Page
INTRODUCTION	1
LASER GENERATED ULTRASOUND	6
LASER INTERFEROMETRIC DETECTION OF ULTRASOUND	9
NONDESTRUCTIVE EVALUATION OF COMPOSITES	12
ACOUSTO-ULTRASONICS	16
EXPERIMENTAL APPARATUS	20
EXPERIMENTAL TESTS AND RESULTS	34
CONCLUSIONS	75
REFERENCES	76

LIST OF FIGURES

		Page
Figure 1.	Basic configuration of bulk-optic path-stabilized interferometer.	21
Figure 2.	Basic configuration of fiber-optic heterodyne interferometer.	23
Figure 3.	Block diagram of phase-locked loop control electronics.	27
Figure 4.	Photograph of compact pulsed laser generator and fiber-optic heterodyne interferometer detector used in ultrasonic transmission mode.	30
Figure 5.	Photograph of fiber-optic heterodyne interferometer detector with cover removed.	31
Figure 6.	Photograph of compact pulsed laser generator and fiber-optic heterodyne interferometer detector used in acousto-ultrasonic mode.	32
Figure 7.	Close-up view of graphite/epoxy acousto-ultrasonic test specimen.	33
Figure 8.	Experimental arrangement for acoustic emission test.	35
Figure 9.	Theoretically predicted vertical surface displacement versus time record for a step-function time dependence point source load applied to the surface of a homogeneous isotropic linear elastic half-space.	37
Figure 10.	Experimentally measured vertical surface displacement versus time record detected with the fiber-optic heterodyne interferometer.	38

Page

Figure 11. Schematic diagram of experimental arrangement to detect ultrasonic pulses generated from a 5 MHz piezoelectric transducer coupled to the bottom of a 3 inch thick 2024 T4 aluminum block 40

Figure 12. Ultrasonic waveform detected using experimental arrangement shown in Figure 11. 41

Figure 13. Ultrasonic waveform detected using experimental arrangement shown in Figure 11 (longer time record). 42

Figure 14. Fast Fourier Transform of 5 MHz ultrasonic pulse obtained using experimental arrangement shown in Figure 11. 43

Figure 15. Schematic of experimental arrangement for pulsed laser generation and path-stabilized interferometer detection of ultrasonic waves passing through a brass plate. 45

Figure 16. Pulsed laser generated path-stabilized laser interferometer detected waveform of ultrasonic wave passing through brass plate. 46

Figure 17. Pulsed laser generated piezoelectric transducer detected waveform of ultrasonic wave passing through same brass plate as in Figure 16. 47

Figure 18. Schematic of experimental arrangement for pulsed laser generation and path-stabilized interferometer detection of ultrasonic waves passing through an aluminum block. 49

Figure 19. Theoretical surface displacement for pulsed laser generated ultrasound in aluminum block detected on epicenter. 51

Page

Figure 20. Surface displacement for pulsed laser generated ultrasound in aluminum block detected by path-stabilized interferometer on epicenter, 52

Figure 21. Waveform obtained for pulsed laser generated ultrasound in aluminum block detected by 2.25 MHz piezoelectric transducer on epicenter. 53

Figure 22. Theoretical surface displacement for pulsed laser generated ultrasound in aluminum block detected 7/8 in (22 mm) off epicenter. 55

Figure 23. Surface displacement for pulsed laser generated ultrasound in aluminum block detected by path-stabilized interferometer at the 7/8 in (22 mm) off epicenter position. 56

Figure 24. Waveform obtained for pulsed laser generated ultrasound in aluminum block detected by 2.25 MHz piezoelectric transducer at the 7/8 in (22 mm) off epicenter position. 57

Figure 25. Diagram showing the geometrical arrangement for acousto-ultrasonic tests. 59

Figure 26. Geometrical shape and dimensions of acousto-ultrasonic specimens. 61

Figure 27. Pulsed laser generated fiber-optic heterodyne laser interferometer detected waveform for the graphite/epoxy 90 degree laminate specimen. 63

Figure 28. Pulsed laser generated conical point piezoelectric transducer detected waveform for the graphite/epoxy 90 degree laminate specimen. 64

Figure 29. Pulsed laser generated fiber-optic heterodyne laser interferometer detected waveform for the graphite/epoxy cross-ply laminate specimen. 66

Page

Figure 30. Pulsed laser generated point conical piezoelectric transducer detected waveform for the graphite/epoxy cross-ply laminate specimen. 67

Figure 31. Pulsed laser generated fiber-optic heterodyne laser interferometer detected waveform for the filament wound composite specimen. 69

Figure 32. Pulsed laser generated conical point piezoelectric transducer detected waveform for the filament wound composite specimen. 70

Figure 33. AET 206 AU unit detected waveform for the graphite/epoxy 90 degree laminate specimen. 72

Figure 34. AET 206 AU unit detected waveform for the graphite/epoxy cross-ply laminate specimen. 73

Figure 35. AET 206 AU unit detected waveform for the filament wound composite specimen. 74

INTRODUCTION

Although historically nondestructive techniques have been used almost exclusively for detection of macroscopic defects in structures after they have been in service for some time, it has become increasingly evident that it is both practical and cost effective to expand the role of nondestructive evaluation to include all aspects of materials production and application. Currently efforts are directed at developing and perfecting nondestructive evaluation techniques which are capable of monitoring and controlling the materials production process; the materials integrity following transport, storage, and fabrication; and the amount and rate of degradation during the materials in-service life. Among the various nondestructive evaluation techniques, ultrasonics plays a prominent role because it affords very useful and versatile nondestructive methods for evaluating the microstructures, associated mechanical properties, as well as micro- and macroscopic flaws in solid materials.

Ultrasonic Waves in Solid Materials

The use of ultrasonic waves as nondestructive probes has as a prerequisite the careful documentation of the propagational characteristics of the ultrasonic waves themselves [1]. Since in nondestructive evaluation applications it is not desirable for the ultrasonic waves to alter the material through which they pass, it is necessary to work with very low amplitude waves, which normally are regarded to obey linear elasticity theory. Although most practical uses of ultrasonics are applied to solid materials which are polycrystalline aggregates and therefore assumed to be isotropic, with real crystalline solids and composites the condition of ideal isotropy is extremely difficult, if not impossible, to attain.

Linear Elastic Wave Propagation

In general three different linear elastic waves may propagate along any given direction in an anisotropic material. These three waves are usually not pure modes since each wave generally has particle displacement components both parallel and perpendicular to

the wave normal. However, one of these components is usually much larger than the other; the wave with a large parallel component is called quasi-longitudinal while the waves with a large perpendicular component are called quasi-shear. In the event that the material is isotropic, then all modes become pure modes, i.e. the particle displacements are either parallel or perpendicular to the wave normal, and the two quasi-shear modes degenerate into one pure shear mode. Also of great practical importance to elastic wave propagation in anisotropic materials is the fact that the direction of the flow of energy per unit time per unit area, the energy-flux vector, does not in general coincide with the wave normal as it does in the isotropic case, i.e. the ultrasonic beam exhibits refraction even for normal incidence.

Attenuation of Nearly Linear Elastic Waves

For all real solids, the assumption of pure linear elasticity is only an approximation, since all real ultrasonic waves are attenuated as they propagate. If one considers this more realistic case, one finds, to the lowest order of approximation, that the general propagational characteristics of such waves in solid materials are identical with the linear elastic case as regards wave speeds, particle displacements, energy flux vectors, and diffraction spread. However, as a result of various mechanisms, there will be energy loss from these propagating waves.

Although geometrical effects can cause energy to be lost from the ultrasonic beam, such losses are not indicative of intrinsic loss mechanisms associated with the microstructure. Once proper precautions are taken to either eliminate or control these geometrical effects, ultrasonic attenuation measurements serve as a very sensitive indicator of internal loss mechanisms caused by microstructures and microstructural alterations in the material [2]. This sensitivity derives from the ability of ultrasonic waves of the appropriate frequency to interact with a variety of defects including cracks, foreign particles, precipitates, porosity, fiber breaks, delaminations, disbonds, voids, grain boundaries, interphase boundaries, and even dislocations.

Nonlinear Elastic Wave Propagation

Nonlinear effects associated with ultrasonic wave propagation may also be used to advantage for nondestructive materials characterization [1]. Nonlinear effects in elastic wave propagation may arise from several different causes. First, the amplitude of the elastic wave may be sufficiently large so that finite strains arise. Second, a material, which in its undeformed state behaves in a linear fashion, may behave in a nonlinear fashion when infinitesimal ultrasonic waves are propagated, provided that a sufficient amount of external static stress or internal residual stress is superimposed. Finally, the material itself may contain various energy absorbing mechanisms such that it is locally nonlinear, e.g. the defects enumerated previously.

Nonlinear elastic waves differ from linear elastic waves in several important aspects. An initially sinusoidal nonlinear longitudinal elastic wave of a given frequency distorts as it propagates, and energy is transferred from the fundamental to the harmonics that appear. The degree of distortion and harmonic generation is directly dependent on the amplitude of the wave. A pure mode nonlinear longitudinal nonlinear wave may propagate alone, but a pure mode nonlinear transverse wave cannot propagate without the existence of an accompanying longitudinal wave. On the other hand, a nonlinear transverse wave does not distort when it propagates in a defect free solid. Nonlinear elastic waves can interact with other waves in the solid. At the intersection of two ultrasonic beams, additional ultrasonic beams can be generated. Interaction with thermal vibrations causes energy loss from the wave. The degree of interaction in all cases is directly dependent on the amplitude of the wave.

Ultrasonic Waves in Inhomogeneous Materials

Additional problems arise with ultrasonic wave propagation in inhomogeneous materials. The presence of a single bounding surface complicates the propagational characteristics of ultrasonic waves in solid materials and can lead to erroneous interpretation of velocity and attenuation measurements. The presence of many bounding surfaces, such as occur in grossly porous or large grain ceramics and in composites, complicates the propagational characteristics even

more and, except in a few special cases, the problems have not been solved analytically. However, solution of these problems will permit proper ultrasonic measurements to be an invaluable tool in characterizing ceramic and composite materials.

Contact or Water Coupled Transducers

Historically, piezoelectric crystals such as quartz were predominantly used as transducer materials. Currently, poled ferroelectric ceramics are most often used. A major problem associated with conventional ultrasonic techniques is the requirement that both the generating and receiving transducers be acoustically bonded to the test material with some sort of acoustical impedance matching coupling medium such as water, oil, or grease; or often more harmful, particularly to porous ceramics or polymer based composite materials, is the necessity of immersing the entire material structure to be tested in a tank of water or coupling the transducers to the workpiece using water squirter systems. Although the couplant allows acoustical energy to propagate into the test material, it causes several problems in addition to potential harm to the material. For velocity measurements the coupling medium can cause transit time errors on the order of one percent of the measured values. Due to partial transmission and partial reflection of the ultrasonic energy in the couplant layer, there may be a change of shape of the waveform which can further affect velocity measurement accuracy. This can also lead to serious errors in absolute attenuation measurements of up to twenty percent of the measured values. This latter fact is the reason that so few reliable absolute measurements of attenuation are reported in the scientific literature. The requirement of physical contact between transducer and test structure places limitations on ultrasonic testing in structural configurations which possess geometries with difficult to reach areas. Limitations are also placed on the testing of materials at elevated temperatures or in the environment of outer space.

It is also important to note that the character of the piezoelectric transducer itself exerts a major influence on the components of the ultrasonic signal, since conventional transducers do not respond as a simple vibrating piston and have their own frequency, amplitude, and directional response. In addition, they "ring" at their resonance frequency and it is extremely difficult to distinguish between the amplitude excursions caused by this

"ringing" and the amplitude variations actually characteristic of the ultrasonic signal. They are also limited in their frequency response and, since they are in contact with the surface of the material to be tested, they can load this surface and thereby modify the ultrasonic wave itself.

Non-Contact Transducers

Because of the limitations of contact transducers, a method of non-contact generation and detection of ultrasound is of great practical importance. Several such techniques are presently available in various stages of development, namely capacitive pick-ups, electromagnetic acoustic transducers (EMAT'S), and laser beam optical generators and detectors. However, as the name implies, capacitive pick-ups cannot be used as ultrasonic generators and, even when used as detectors, the air gap required between the pick-up and test structure surface is extremely small, which in essence causes the device to be very nearly a contact one. EMATs, on the other hand, have already been successfully used for material defect characterization particularly in metal bars, tubes, pipes, and plates. They have also been used for metallic property measurement such as material anisotropy (texture) and internal stress (strain) state. One major problem with EMATs is that the efficiency of ultrasound generation and detection rapidly decreases with lift-off distance between the EMAT face and the surface of the test object, as well as with increasing temperature of the test material. They can obviously only be used for examination of electrically conducting materials and, therefore, cannot be used for examination of non-conducting ceramics and composites. Laser beam ultrasound generation and detection overcomes all of these problems and affords the opportunity to make truly non-contact ultrasonic measurements in both electrically conducting and non-conducting materials, in materials at elevated temperatures, in corrosive and other hostile environments, in geometrically difficult to reach locations, in outer space, and do all of this at relatively large distances, i.e. meters, from the test object surface.

LASER ULTRASOUND GENERATION

As early as 1963, White [3] reported the generation of elastic waves in solid material by transient surface heating and research has continued in this area up to the present time [4-14]. Three different mechanisms have been proposed to account for the generation of ultrasonic waves by the impact of laser pulses, namely radiation pressure, ablation, and thermoelasticity. Radiation pressure, which is caused by momentum transfer from the incident electromagnetic pulse, is the least efficient of the three proposed mechanisms and is therefore of little importance for practical applications.

At the other extreme, when a laser pulse possessing sufficient power density strikes the surface of a material the electromagnetic radiation is absorbed in a very thin layer of the material and vaporizes it. The amplitude of the ultrasonic wave generated in the material by this ablation process can often be increased by placing a coating of a material possessing different thermal properties on the surface of the test object. The use of a constraining layer may yield larger amplitude signals at certain detection sites without causing damage to the material being tested.

Although the surface of the test object is slightly damaged when ablation occurs, in certain cases the amount of damage is acceptable when such a generation process is the only way to obtain ultrasonic waves of sufficient amplitude in a non-contact manner. Stresses normal to the surface are set up resulting from momentum transfer when ablation occurs. At very high laser power densities, the stresses caused by the momentum transfer when ablation occurs may become quite large and may greatly affect the ultrasonic waves which are generated, whereas for lower ablating powers, momentum transfer plays a smaller role in the generation of ultrasonic waves, and the thermoelastic mechanisms dominate. For nondestructive evaluation, one would want to remain in the thermoelastic regime in order to avoid material ablation.

The thermoelastic process consists of absorption of radiation from a laser pulse possessing moderate energy in a finite depth of the material under investigation. As radiation is absorbed, the material heats up and expands. This expansion and subsequent contraction of the material in the area excited by the laser pulse leads to the generation of elastic waves in the material. Thus, the

thermoelastic process is the only process which is truly nondestructive and still capable of generating an ultrasonic wave of sufficient amplitude for nondestructive evaluation purposes.

The ultrasonic waves generated by a laser pulse depend heavily on the absorption coefficient of the material with respect to the wavelength of the radiation from the source laser. A material with a low absorption coefficient will have a larger interaction volume with the radiation than a material with a high absorption coefficient. Thus the interaction volume for a material with a very high absorption coefficient would resemble a disk, while a material with a very low absorption coefficient would have an interaction volume which is more like a cylinder.

Thermoelastic generation at a free surface of a solid material results from pressure release at the surface. The major stresses which are set up because of the laser pulse and subsequent thermal expansion of the material are parallel to the surface, and thus most of the ultrasonic energy propagates radially from the area of laser excitation.

Generation at a constrained surface can lead to an increase in ultrasonic energy propagating normal to the material surface. By constraining the surface, stresses normal to the surface are set up. If the constraining layer is a thin layer of oil or other similar substance, stresses normal to the surface are set up resulting from momentum transfer if the constraining layer evaporates. A rigid constraining layer will lead to large stresses which are set up normal to the surface due to thermal expansion since the constraining layer leads to a reduction in stress release at the surface of the material.

One factor which may lead to an increase in the use of laser generation deals with the frequencies of the ultrasound which are generated by laser pulses. The ultrasound generated by lasers is generally quite broad band in frequency content, and the energy may be propagated predominantly in certain directions because of the conditions at the surface of the material. By narrowing the bandwidth of the laser generated ultrasound, detection devices with bandwidth dependent sensitivities such as laser interferometers will benefit greatly. Several papers dealing with narrowing the bandwidth of laser generated ultrasound have been presented [15,16]. Also since specific frequencies are used in certain

applications, the ability to generate those frequencies using lasers would greatly enhance the usefulness of this source of ultrasound.

The use of lasers to generate ultrasound in a material can therefore be seen to differ from the use of piezoelectric transducers in several important ways. Lasers are non-contact and thus problems associated with contact transducers, such as contact pressure and other coupling problems, are eliminated. This allows testing on surfaces hostile or inaccessible to piezoelectric or other contact transducers. The laser used to generate the ultrasound may be placed at a considerable distance from the material to be tested. Laser generation is usually broader band in frequency content, and the resulting waves will depend largely on the characteristics of the material and the conditions of the surface of the material.

LASER INTERFEROMETRIC DETECTION OF ULTRASOUND

Initial work with laser generation of ultrasound was performed using piezoelectric transducers as detectors since the various investigators had prior experience with this type of transducer and associated electronic equipment. More recently a number of investigators have used laser beam interferometers for non-contact detection of acoustic emission and ultrasonic waves in solid materials [17-22]. Non-contact detectors of ultrasound such as laser interferometers offer several advantages over contact transducers such as piezoelectric transducers.

First of all, since only a light beam contacts the surface of the material being tested, contact pressure can be neglected and thus the surface will not be loaded. The problem of contact pressure associated with the use of piezoelectric transducers is therefore eliminated. Since no mechanical contact is required for the interferometer to detect the displacement of a material surface, there is no need for the use of a coupling medium, and all of the problems associated with the use of coupling media are eliminated. This is important since the detector is always looking directly at the surface being tested, and not detecting a waveform which is arriving indirectly from the material surface via some coupling medium. There is also the possibility of sending the probe beam through a transparent material in order to probe inside the transparent material as well as a surface which is behind the transparent material.

Interferometers may also be used to detect ultrasound on surfaces which are hostile to piezoelectric transducers, such as surfaces which are at elevated temperatures or in corrosive environments. The interferometer may also be placed at a considerable distance from the material to be tested since only the probe beam needs to contact the surface of the material, and thus the interferometer may be shielded from possible hostile environments near the testing site.

The area of the probe beam of the laser interferometer may be varied using focussing optics. The probe beam may be focussed down to a spot several microns in diameter which may be advantageous in certain applications. Focussing down to a small spot eliminates phase effects associated with piezoelectric transducers

that have large active detection areas. The waveform obtained from an interferometer which has been focussed down to a small spot is therefore a record of the displacement of that small area of the material surface, and not of some large area which may be larger than the wavelength of the ultrasound which is propagating through the material. The small area of the probe beam may also make it possible to use interferometers in areas inaccessible to large area piezoelectric transducers such as in cavities and near material edges. Detection of ultrasound on curved surfaces is also possible when using a laser interferometer having a small area probe beam.

Another major advantage in using laser interferometers instead of piezoelectric transducers for the detection of ultrasound is that laser interferometers are free of the mechanical resonances which affect the response of many piezoelectric transducers. This absence of mechanical resonance enables the interferometer to be equally sensitive to all components over a broad frequency band. Since there is no coloring by the interferometer, the waveform received reflects the true displacement of the surface of the material over the time of the waveform.

Yet another advantage in using a laser interferometer involves the fact that the amplitude of the surface displacement can be determined from the output waveform. By measuring the peak-to-peak voltage for a full-fringe displacement, the fractional fringe displacement resulting from the ultrasound can be found, and since the wavelength of the light is known, the amplitude of the surface displacement can be calculated. Since the interferometer is equally sensitive to all of the frequencies in its bandwidth, all displacements can be determined.

There are, however, several important disadvantages associated with the use of laser interferometers for the detection of ultrasound. The sensitivity of the interferometer is strongly dependent on the amount of light which comes back from the material surface. The material surface must be capable of reflecting a sufficient amount of laser light back to the interferometer to match the intensity of the laser light in the reference beam. The material surface must therefore be reflective and fairly smooth in order to allow the interferometer to approach its maximum sensitivity. However, even with a finely polished, highly reflective surface, the sensitivity of currently available interferometers is usually not as high as that of piezoelectric transducers. Many interferometers are

also subject to the ambient vibrations in testing areas and may therefore need some kind of correction circuit in order to separate the ultrasonic displacements from the signals due to the ambient vibrations. Also, proper alignment of the interferometer with the surface to be tested may be difficult to attain and may be easily destroyed.

NONDESTRUCTIVE EVALUATION OF COMPOSITES

The term composite covers a wide variety of materials, including boron/epoxy, glass/epoxy, graphite/epoxy, Kevlar/epoxy, and silicon carbide fiber reinforced silicon carbide matrix. Nondestructive evaluation of composite materials is appreciably more complex than nondestructive evaluation of monolithic metals and ceramics primarily because of the types of defects causing failure of each material. In metallic and ceramic materials the predominant failure causing flaws are cracks and those discontinuities which may lead to crack initiation and growth. In composites, the material integrity may be adversely affected by improper cure, inclusions, voids, porosity, environmental degradation, machining damage, impact damage and fretting. A number of nondestructive evaluation techniques which have been well-developed for use with other materials have also been successfully used to monitor composites. In addition, some techniques uniquely applicable to particular composites have shown promise. A number of review articles have been published concerned with nondestructive evaluation of composites [23-41].

Ultrasonic techniques have been used much more than any other nondestructive method to investigate composite materials. Among these ultrasonic techniques pulse-echo or pulse-transmission procedures have been used most often in the conventional contact, water immersion or water squirter modes to measure velocity and attenuation and thereby determine the associated mechanical properties. These techniques have been used to detect voids [38,42,45-50,60], inclusions [50.51,62,63], disbonds [28,50], cracks [39,53,59], delaminations [34,38,48,50,60], cure [43], lay-up order [52], fatigue life [53], fiber orientation [50], residual strength [23,34,44,54-58,64], and resin-starved areas [30,61].

In addition to ultrasonics, attention has been given to radiography, thermal techniques, electrical measurements, acoustic emission, optical fibers, visual inspection, dye penetrants, tap testing, and vibrational methods. Although most of the radiographic techniques performed to date have been with x-rays, neutron radiography has also been used successfully. Since many composites are low absorbers of x-rays, it is necessary to work with low energy radiation in the 10 -50kV range obtained with a beryllium window x-ray tube. Most modern techniques which are striving for high

resolution images apply microfocus x-ray machines, which possess an extremely small focal spot, and a long source to film distance. The types of defects detectable with x-ray radiography are porosity, inclusions, voids, and properly oriented cracks and delaminations. Addition of x-ray opaque liquid, which penetrates into the defects, increases the probability of detection of cracks, delaminations, fatigue damage, fiber breakage, and matrix crazing.

Since many composite materials are either entirely or partially composed of polymers, they possess much lower thermal conductivity than metals and consequently any temperature distribution created in such a composite will be relatively easily detected on the surface of the specimen. Thermographic techniques are both passive and active. Passive techniques are those in which heat is supplied to the surface of the test specimen from an external source, such as a hot plate, a heat gun, or an intense light, and defects in the specimen are indicated by changes in the observed temperature differences of the test specimen surface. Passive thermographic techniques have been successfully used to detect debonds, delaminations, porosity, and voids. Active techniques are those in which heat is generated by application of mechanical vibration to the test specimen and conversion of this mechanical vibration into heat by frictional processes at the defects. These techniques have successfully detected cracks, debonds, and delaminations.

Dielectric and eddy current measurements are the primary electrical techniques used to nondestructively inspect composite materials. Dielectric techniques, which are limited to use with electrically insulating materials, have been primarily used to monitor the curing of glass and polymer based composites. Eddy current techniques have been primarily used with graphite fiber and metal matrix composites, since this technique requires the composite to be an electrical conductor.

Acoustic emission has been used successfully to monitor the creation and enlargement of defects in composite materials. Although generally categorized as a nondestructive testing technique, acoustic emission testing is not totally nondestructive, since the test structure must be subjected to either an external mechanical or thermal load in order to observe the acoustic emission signals. The acoustic emissions detected result from a sudden release of elastic energy due to relieving of this externally applied load by either

creation or movement of the defects. Acoustic emission techniques have been successfully used to detect debonding, fracture of fibers, and fiber pull-out. The ultimate success of this technique often depends on the validity of what is known as the Kaiser Effect, in which no acoustic emissions are observed on a previously loaded structure until that load level is reached which exceeds the load applied to the test structure during the immediately preceding test period.

An optical fiber interferometric technique has been used to inspect graphite fiber reinforced composites by measuring fringe shifts caused by dimensional changes in the optical fibers. This technique requires an optical fiber being embedded in the composite material and an identical fiber being isolated from the test specimen. Strains present in the structure cause a change in the embedded optical fibers dimension. Comparison of the light passing through the strained embedded fiber with that passing through the strain-free isolated fiber results in a measurable phase shift, which can be related to the strain difference in the fibers by appropriate calibration procedures. A different technique involving optical fibers is to embed one of more rectangular grids of optical fibers in the composite test structure. By choosing the fibers used so that their failure load is as close as possible to the failure load of the fibers in the composite test structure, the optical fibers will fracture at the same load level as the fibers in the composite. The optical fiber breakage is monitored by observing the lack of transmission of light through it. The intersection of the orthogonal broken fibers in the rectangular grid locates the damaged region. The unique feature of these optical fiber techniques for nondestructive testing is that the monitoring devices, the optical fibers, are an integral part of the structure, thus resulting in a built-in sensor array.

The visual techniques utilize transmission or reflection of light. For translucent materials variations in the intensity of transmitted light serves as an indication of internal structural alterations. In the case of opaque composites, light is incident at an oblique angle on the surface to be inspected and the presence of surface discontinuities are enhanced when subsequently viewed from normal and oblique angles. This technique has been used to detect matrix cracking, surface delaminations, gouges, dents, and abrasive wear.

Conventional liquid dye penetrant inspection is often used to inspect composites, particularly where it is necessary to inspect large

areas rapidly. This technique has been used to detect cracks and other surface discontinuities such as edge delaminations and porosity.

Tap testing is somewhat of a classical technique which requires application by a person experienced with the technique. This technique uses a special tapping hammer, coin, or other metallic object to lightly tap the test structure. Alterations in the composite structure are detected as changes in the audible sounds by the inspector. Delaminations, resin softening, and internal damage have been detected by this technique.

Vibrational techniques are based on monitoring the lowest natural resonance frequency of the composite test specimen. The state of damage is reportedly detected as a change in this natural frequency due to a reduction in the stiffness caused by local defects. Among the types of damage reportedly determined are crushing, three-point bend loading damage, cuts, impact damage, and holes. This technique, although potentially promising, has not been extensively investigated and the test results have not been sufficiently substantiated.

ACOUSTO-ULTRASONICS

As early as 1975, Vary [65,66] showed the feasibility of ranking material fracture toughness by ultrasonic attenuation measurements. He and his colleagues presented additional empirical evidence for the close relation that exists between ultrasonic velocity and attenuation values and the mechanical properties of composite materials [67-71], and between ultrasonic attenuation values and fracture toughness properties of metals, ceramics, and composites [72-74]. The model he suggested, as a theoretical basis for the empirically related correlations that were found between ultrasonic propagation and fracture toughness properties of metallic materials, was based on stress (elastic) wave interactions during microcracking and void coalescence [75]. In subsequent publications these concepts were further expanded upon and new experimental evidence for their validity was presented [76-88].

Based on the results of the previously referenced authors, the acousto-ultrasonic method has attributes that make it practical for assessing mechanical properties of highly inhomogeneous, anisotropic materials. The acousto-ultrasonic method, also referred to as the stress wave factor method or technique, is a modification of the ultrasonic pulse-echo method, but differs from it in several important aspects. First, in its original form, two transducers possessing different frequency characteristics were used. The generator transducer was a conventional ultrasonic transducer operating typically in the 1 - 10 MHz regime, while the receiver transducer was typically a conventional acoustic emission transducer operating in the 100 - 150 kHz regime. Acousto-ultrasonic tests are now run with various types of transducers and the receiving transducers used are no longer limited to the 100-150 kHz regime. The choice of frequency regime is often determined by the geometry and type of sample being tested. Second, the transducers are coupled to the same surface of the test material in such a manner that the receiving transducer cannot receive a direct set of pulses from the generating transducer. In a few examples, through transmission has been reported, but the majority of acousto-ultrasonic tests are run with both the generating and receiving transducers coupled to the same side of the material which is under test. Third, the received signals are considerably more complex than those normally obtained with conventional pulse-echo testing and, therefore, require more elaborate electronic processing.

Analysis of acousto-ultrasonic signals is accomplished by measurement of the Stress Wave Factor (SWF). The SWF may be measured in several ways in order to assign a numerical value to the acousto-ultrasonic waveform. For example, the SWF may be evaluated in a similar fashion as is done in normal acoustic emission signal analysis, namely as either a "ringdown" oscillation count or as the root-mean-square (RMS) voltage of the output waveform. In the frequency domain, the SWF may be evaluated in terms of the power spectrum or spectral features that change with material factors.

Although it was originally applied to composite materials, the acousto-ultrasonic technique has since been used on various non-engineered materials, including wood products [89-91], and bone [92], as well as wire rope [90], nylon rope [93], and glass ceramics [94]. The use of the acousto-ultrasonic technique for the nondestructive evaluation of adhesive bonds has been reported by a number of investigators [90,95-97]. Several authors [85-88,98,99] have written critical assessments of the acousto-ultrasonic technique as a nondestructive evaluation technique for composite materials citing concerns which must be closely watched. Of major concern has been the reproducibility of the test conditions, and the effects of the test equipment.

In a series of reports [85-88], researchers at Virginia Polytechnic Institute and State University related their study of the acousto-ultrasonic technique for the characterization of composite materials. The reports, spanning from 1983 to 1989, show the evolution of the acousto-ultrasonic technique. In the early reports, an AET 206 AU unit was used to run the acousto-ultrasonic tests. The AET 206 AU is a commercial acousto-ultrasonic unit which gives a value for the SWF. In later reports, the AET 206 AU unit was no longer used, and various piezoelectric transducers with differing characteristics were used. The researchers also discussed the feasibility of using a Nd:YAG laser to generate the acoustic events for acousto-ultrasonic tests, while citing the need for non-contact generation and detection in the acousto-ultrasonic technique for certain applications.

The acousto-ultrasonic technique has been used by many authors for the detection of damage and damage development in composites [100-105]. It has also been used to monitor the manufacture of composites for quality control [104], and it has been

used for the prediction of damage development in composite materials [106]. Acousto-ultrasonics has been used to assess crack density in composite materials [107].

Phani et al. [108] found the SWF to be a sensitive indicator of strength and porosity for a porous brittle solid such as gypsum. De and Phani [94] found acousto-ultrasonics to be sensitive for monitoring nucleation and crystallization in glass-ceramic systems. Dos Reis and McFarland [89] used acousto-ultrasonics to characterize wood fiber hardboards which were subjected to cyclic soak tests; the SWF was found to decrease with increasing damage. Dos Reis and Kautz [109] applied acousto-ultrasonics in the nondestructive evaluation of adhesive bond strength in rubber-steel adhesive joints, and found that higher SWF values were obtained from bonds with higher values of peel strength obtained in destructive peel strength tests. Brahma and Murthy [110] used acousto-ultrasonics in the evaluation of bimetallic strip bond quality using a through transmission set-up. Kiernan and Duke [111] monitored the anisotropy of fiber-reinforced composite plates as a function of azimuthal angles using acousto-ultrasonics. Kautz [112] investigated the strength of filament wound composite materials through the use of the acousto-ultrasonic technique.

Kautz [113] reported on the use of a pulsed laser to generate ultrasound in composite materials using an acousto-ultrasonic test set-up. He used a pulsed Nd:YAG laser to generate ultrasound in a neat resin, as well as in graphite fiber/polymer composite specimens, and detected the ultrasound with a 1 MHz broad band piezoelectric transducer. He also investigated the damage to the specimens at various Nd:YAG energy levels, and he concluded that the signal levels received by the piezoelectric transducer receiver resulting from laser excitation at energies well below the damage threshold were comparable to the signal levels from waveforms which were generated using piezoelectric transducers.

Sarrafzadeh-Khoee and Duke [114] showing the need for a non-contact detector of ultrasound used a blazed grating Michaelson-type interferometer as an optical detector to detect a piezoelectric transducer generated signal on composite materials which were mirrorized at the laser detection site. In a later report, Sarrafzadeh-Khoee et al. [115] reported the design of a new interferometric detector based on laser speckle. In the most recent report, Duke et

al. [116] asked a number of questions about laser generation and detection of ultrasound.

A number of papers have been published by researchers in the Johns Hopkins University Center for Nondestructive Evaluation already answering these questions [11,12,15-19,22,117-128].

In the present report the use of laser systems for both the generation and detection of acousto-ultrasonic signals is presented for the first time. A laser acousto-ultrasonic test set-up was employed on several composite samples in order to obtain waveforms from this type of experimental set-up, and thereby show the feasibility of using lasers in the acousto-ultrasonic technique for both the generation and detection of ultrasound in materials including composites.

EXPERIMENTAL APPARATUS

Interferometers

Two interferometers were constructed and used to obtain the waveforms reproduced in this report. One of them was a bulk-optic path-stabilized interferometer and the other was a fiber-optic heterodyne interferometer. Figure 1 is a block diagram of the basic configuration for the bulk-optic path-stabilized interferometer. The beam from a helium-neon laser is directed through a beam splitter cube, which splits the incident light into two perpendicular paths. One path is the reference path and the light in this path is directed to a reference mirror. This light is then reflected by the mirror back through the beam splitter cube to the photo-detector. The second light path is the probe path and the light in this path passes through the beam splitter to the surface of the material to be tested. The light reflected from the surface of the material passes back to the beam splitter where it is directed to the photodetector. Interference of the light from the two paths at the photodetector produces the output signal from the interferometer. As with most interferometers, this interferometer is subject to the ambient vibrations of the test site. Therefore, an electronic correction circuit is used to correct for this. The signal from the photodetector is sent through a low pass frequency filter, the output signal of which is used to drive a piezoelectric element attached to the reference mirror. The movement of this mirror removes the low frequencies resulting from the ambient vibrations leaving a signal corresponding to the surface displacements of the material due to the ultrasound travelling through it.

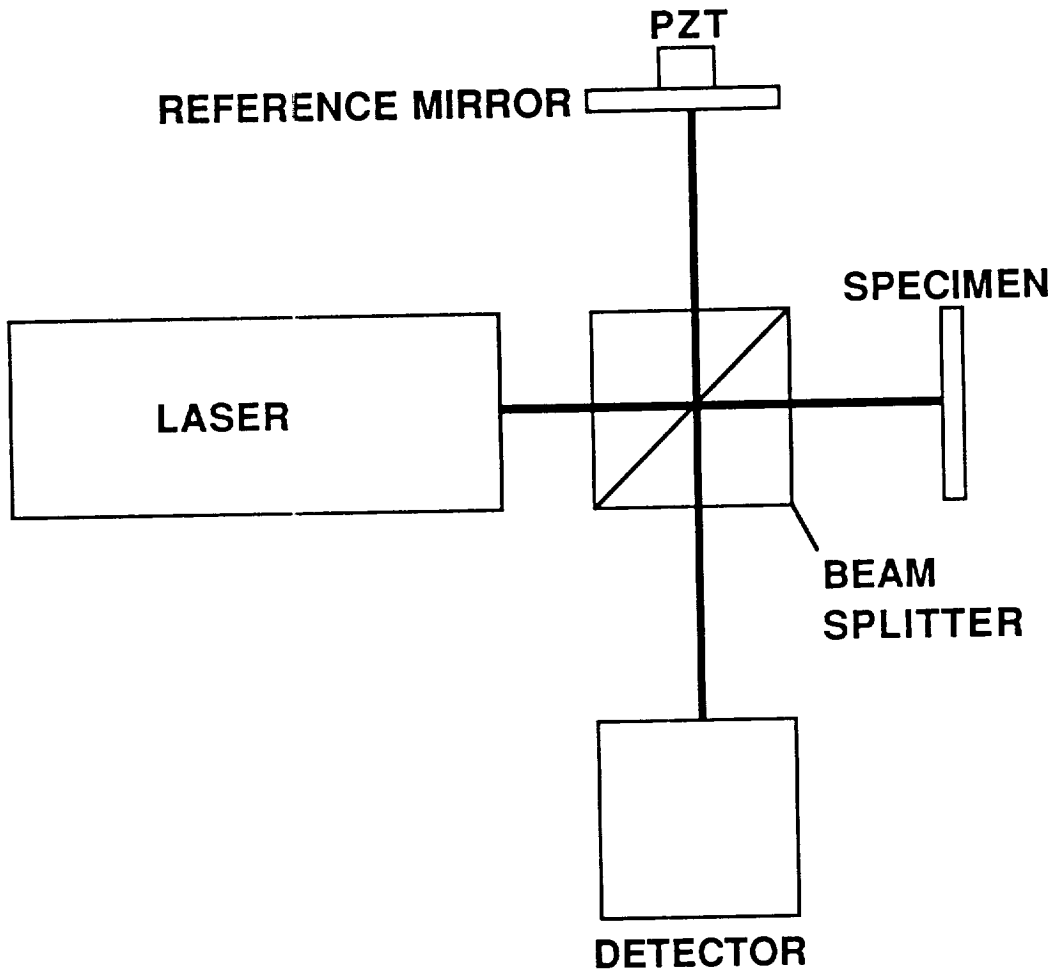

Figure 1. Basic configuration of bulk-optic path-stabilized interferometer.

Figure 2 is a block diagram of the basic configuration of the fiber-optic heterodyne interferometer. A helium-neon laser beam is passed through an acousto-optic modulator, which shifts the frequency of the light such that several orders of light are obtained shifted in frequency by integral numbers of the driving frequency of the acousto-optic modulator. For the interferometer, the zero and first order beams are used. The zero order is unshifted, while the first order is shifted by the drive frequency of the acousto-optic modulator. The interferometer used in the present work employed a first order beam shifted by a frequency of 40 MHz from the zero order beam. The intensities of the light in the two orders was maximized in order to maximize the sensitivity of the interferometer.

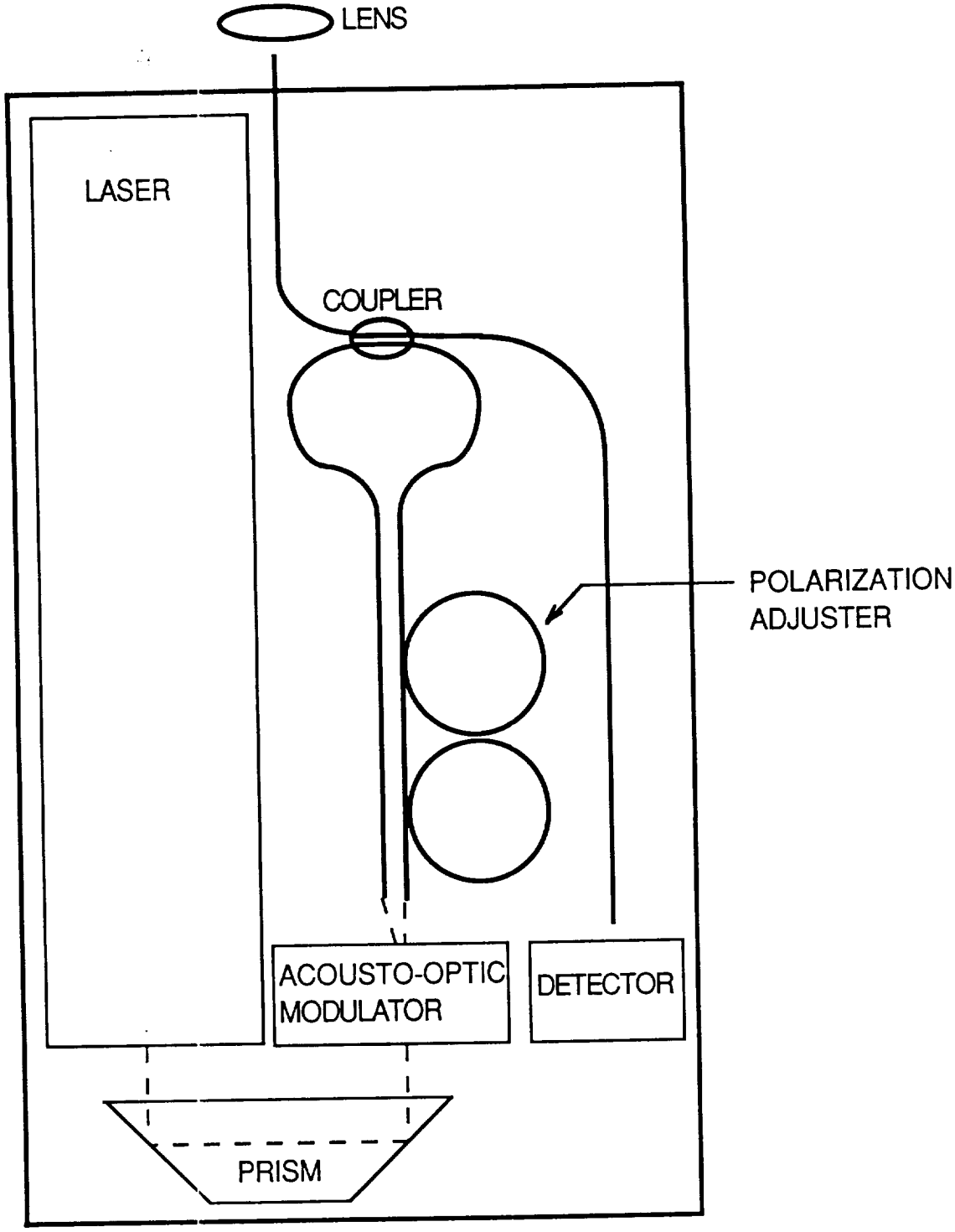

Figure 2. Basic configuration of fiber-optic heterodyne interferometer

The zero and first order beams are then directed into two single mode optical fibers, which lead to two optical paths; a reference path and a probe path. A fiber-optic coupler is used to couple the light to and from the two different paths so that interference of the light from the two paths may occur. Light from the two paths is directed to a photodetector.

When there is no out of plane displacement of the surface which is being probed, the photodetector yields a signal which is at the difference frequency of the two orders of light, namely the drive frequency of the acousto-optic modulator. When there is out of plane displacement of the surface which is being probed, the path length of the probe arm of the interferometer is effectively changed, and this change in path length results in a phase shift of the light at the detector. The signal received from the photodetector thus has the information concerning the displacement of the surface as well as the frequency difference of the two orders of light from the two paths of the interferometer. Therefore, in order to obtain the information corresponding to the surface displacement due to the ultrasonic wave without the frequency components caused by the shift from the acousto-optic modulator, electronic processing of the signal must be implemented. This electronic processing involves the use of an electronic mixer to mix out the frequency shift imposed by the acousto-optic modulator. Control electronics are also used to eliminate noise in the signal which result from ambient vibrations.

There are several advantages in using optical fibers in the design of the interferometer. First of all, it is more convenient to match the path lengths of the two arms of the interferometer using optical fiber since the fiber can be bundled up. This can also make the over-all size of the interferometer more compact. Also, fiber is flexible and affords the possibility of having a small remote probe head which can be manipulated in various positions quite easily. This facilitates the scanning of a material surface by moving only the probe head, and not the entire interferometer. Another advantage of using optical fibers is that the light travelling through the fibers is less sensitive to the temperature and pressure gradients at the testing site, which change the index of refraction of the air in the optical paths.

There are, however, several disadvantages in using optical fibers in the construction of a laser interferometer. One major

disadvantage in using optical fibers is that the sensitivity of a fiber-optic interferometer may be less than that of a bulk system which employs a laser with the same power. The reason for this concerns the problem of coupling the laser light into the optical fibers. Light is lost in the coupling process which leads to a decrease in the amount of light falling on the photo-detector and a corresponding decrease in the maximum sensitivity of the interferometer. Another consideration is the need to maintain the integrity of the fiber ends in order to maximize the coupling of light to and from the fibers. This includes the proper cleaving and care in handling. Since twists and turns in the fibers can lead to changes in the direction of polarization of the light propagating through them, a polarization adjuster is used in one arm of the fiber-optic heterodyne interferometer used in the present work. This polarization adjuster allows the direction of polarization of the light travelling through one of the two fibers to be changed and thereby matched to the polarization of the light in the other fiber, and thus yield an increase in sensitivity. The polarization adjuster is manipulated until the carrier signal, corresponding to the difference frequency of 40 MHz, is maximized at the detector.

Control Electronics

The control electronics of the heterodyne fiber-optic interferometer implements a feedback system in the form of a phase-locked loop in order to eliminate frequencies resulting from room vibrations and other low frequency components which are not caused by the ultrasound propagating through the specimen. A block diagram of the phase-locked loop electronics is shown in Figure 3. A voltage controlled oscillator with a center frequency equal to the drive frequency of the acousto-optic modulator is used. This oscillator outputs a sine wave at its center frequency, but the output frequency can be changed by adjusting its voltage control input. The outputs of the voltage controlled oscillator and the photodetector are input into an electronic mixer, the output of which yields the difference of the two input signals. The mixer output is sent through a low pass filter and the resultant signal is used to drive the voltage controlled oscillator, thereby giving the interferometer its active feedback to eliminate unwanted low frequency components. The cut-off frequency of the low pass filter is on the order of a few kilohertz. This value is high enough to eliminate the low frequencies caused by room vibrations, yet low enough so that it will not affect

the ultrasonic regime of frequencies which are being used to test the material. The voltage controlled oscillator is capable of frequency excursions of a few kilohertz around its center frequency in order that these low frequencies can be tracked and processed out of the signal.

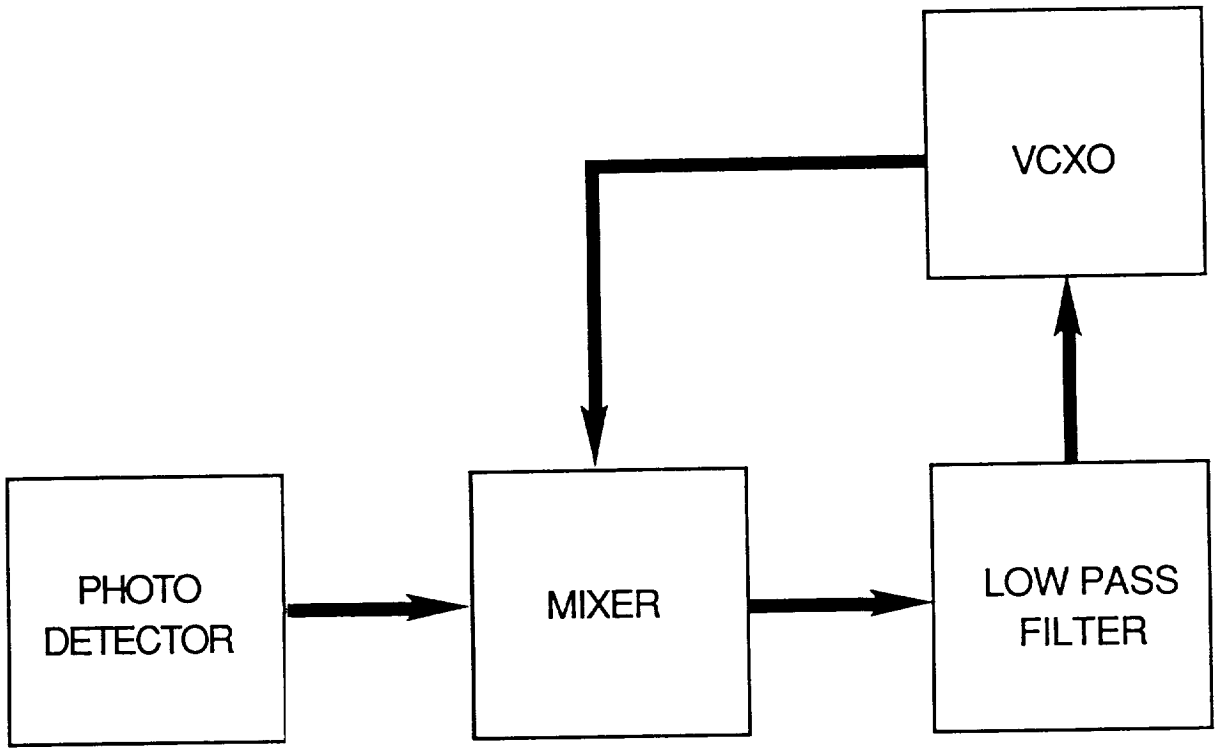

Figure 3. Block diagram of phase-locked loop control electronics.

The output of the mixer is also the output signal of the interferometer. Since the fiber-optic heterodyne interferometer employed an acousto-optic modulator with a drive frequency of 40 MHz, the output of the interferometer has a bandwidth of approximately 20 MHz. The use of a low pass filter on this output increases the signal to noise ratio by reducing the effective bandwidth. If the frequency of the ultrasound travelling through the material being tested is of a known narrow band of frequencies, a band pass filter with a narrow bandwidth centered at the frequency of the ultrasound may be used, and the sensitivity of the interferometer will be greatly enhanced over its broad band sensitivity.

Waveform Recording

The data was captured using a Data Precision Data 6000 waveform analyzer capable of sampling as fast as 10 ns per data point. The waveforms were stored on floppy disk and analyzed using the Data 6000, or a PC. A Kigre model MK-367 pulsed Nd:YAG laser was used for laser generation of ultrasound. This laser has a maximum pulse energy of 17 mJ per pulse, a 4 ns pulse duration, and a 3 mm beam diameter. The MK-367 is air cooled and the laser head is 100 mm long. The compact size of the MK-367 laser made it extremely convenient to use. A PIN diode was used to generate a trigger signal for the laser generated waveforms. The PIN diode detected the laser pulse and the resulting signal from the PIN diode was sent to the waveform analyzer to start the waveform recording. This allowed time-of-flight measurements to be made.

Photographs of Laser Generation/Detection Apparatus

Figures 4 and 5 are photographs showing the laser generation/detection ultrasonic test set-up using the Kigre Nd:YAG pulsed laser to generate the ultrasound and the heterodyne fiber-optic interferometer for detection. The interferometer is shown with (Figure 4) and without its cover (Figure 5). On the right in the foreground, the probe of the interferometer is shown, and the pulsed laser is on the left. The dimensions of the interferometer optics with the cover on are: 18 3/8 inches (46.6 cm) long, 7 5/8 inches (19.4 cm) wide, and 5 1/4 inches (13.2 cm) high. Figure 6 is a photo of the compact pulsed laser generator and fiber-optic heterodyne interferometer detector used in the acousto-ultrasonic mode. A

close-up view of the graphite/epoxy acousto-ultrasonic test specimen is shown in Figure 7. This state-of-the-art laser based acousto-ultrasonic system, incorporating a compact pulsed laser and a fiber-optic heterodyne interferometer, was delivered to the NASA Lewis Research Center along with this final report.

ORIGINAL PAGE
BLACK AND WHITE PHOTOGRAPH

Figure 4. Photograph of compact pulsed laser generator and fiber-optic heterodyne interferometer detector used in ultrasonic transmission mode.

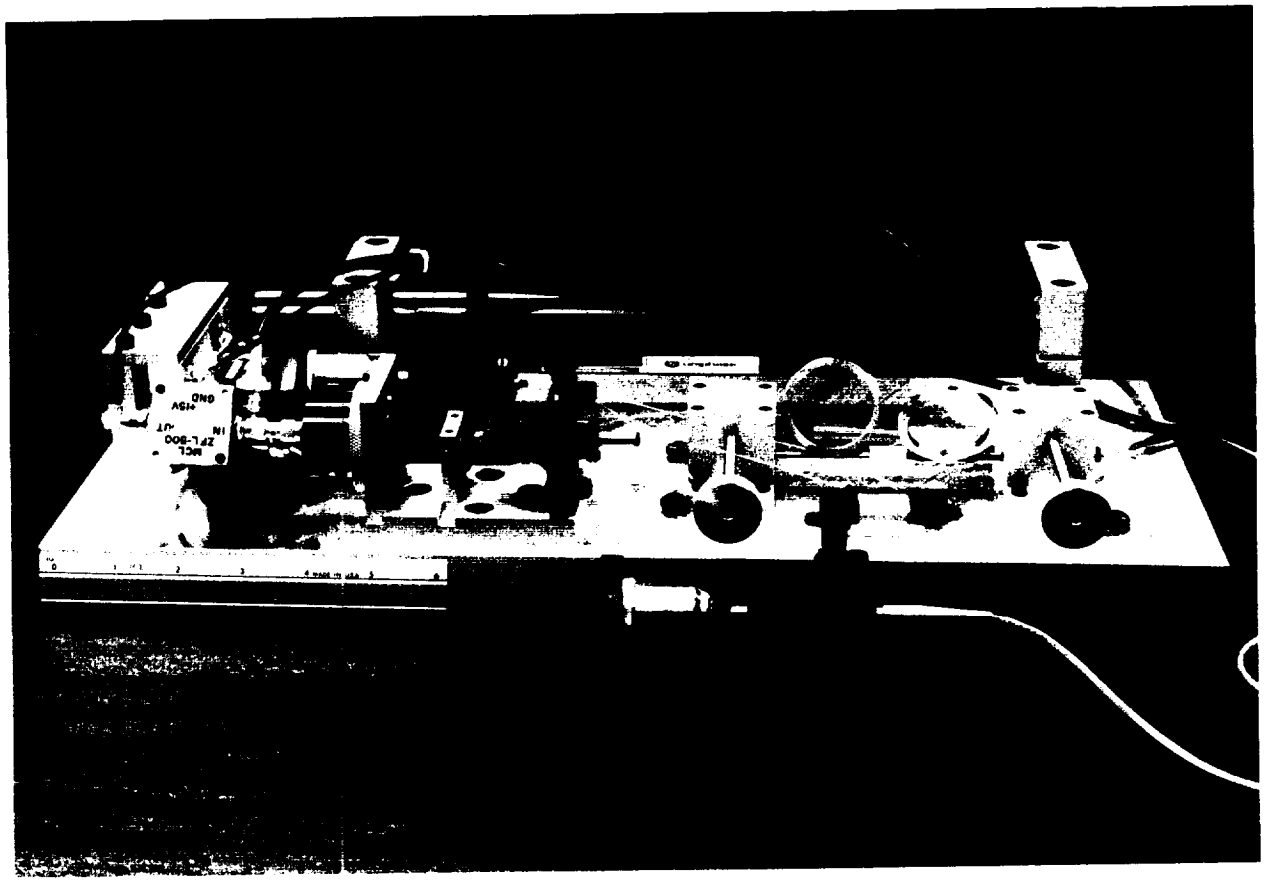

Figure 5. Photograph of fiber-optic heterodyne interferometer detector with cover removed.

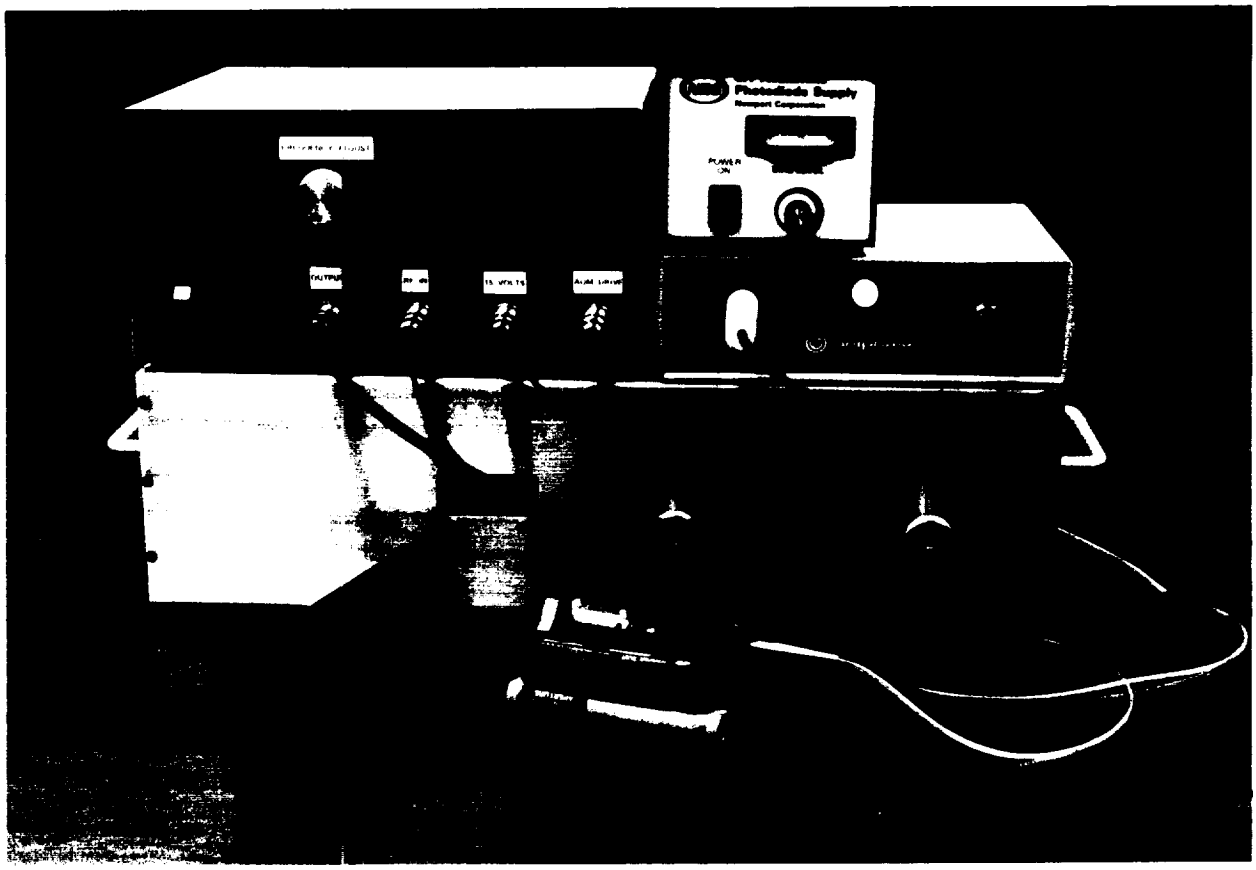

Figure 6. Photograph of compact pulsed laser generator and fiber-optic heterodyne interferometer detector used in acousto-ultrasonic mode.

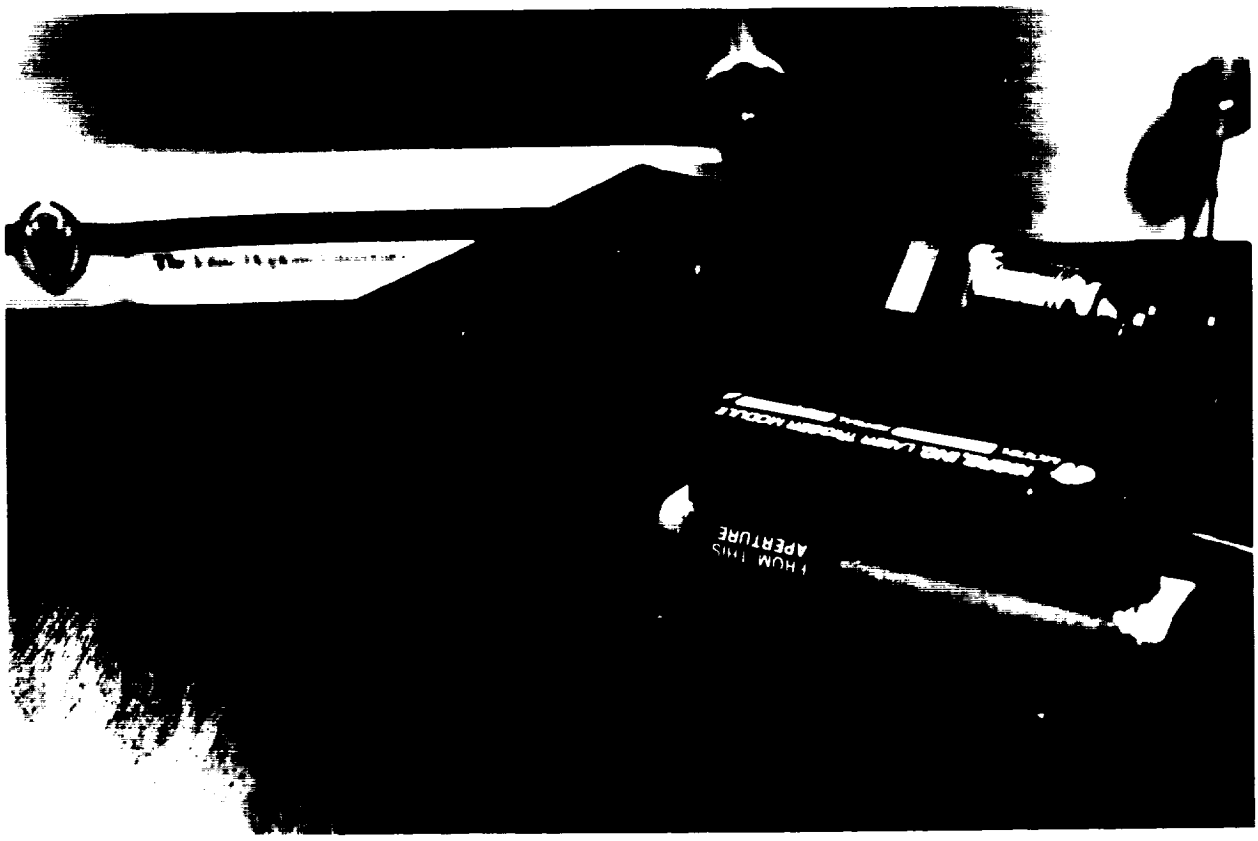

Figure 7. Close-up view of graphite/epoxy acousto-ultrasonic test specimen.

EXPERIMENTAL TESTS AND RESULTS

The data for this report was obtained in a series of tests. Each of the test series consisted of a different test set-up.

Detection of Acoustic Emission Event

In order to check out the original design of the interferometer, tests were made of the surface displacements detected on the same surface of an aluminum test block on which a glass capillary tube was broken. Figure 8 is a diagram of the experimental set-up for this test. A glass capillary was broken on a three inch (76mm) thick aluminum block in such a fashion to simulate an acoustic emission event. The capillaries used had an inner diameter of 0.7mm and an outer diameter of 1.0mm. Each capillary was broken by screwing down a tapered brass indentor on the capillary lying on top of the aluminum block. A piezoelectric disc contained within the brass loading device was used to detect the instant of fracture of the glass capillary and thereby to trigger the data acquisition device to start the recording of the interferometrically detected surface displacement.

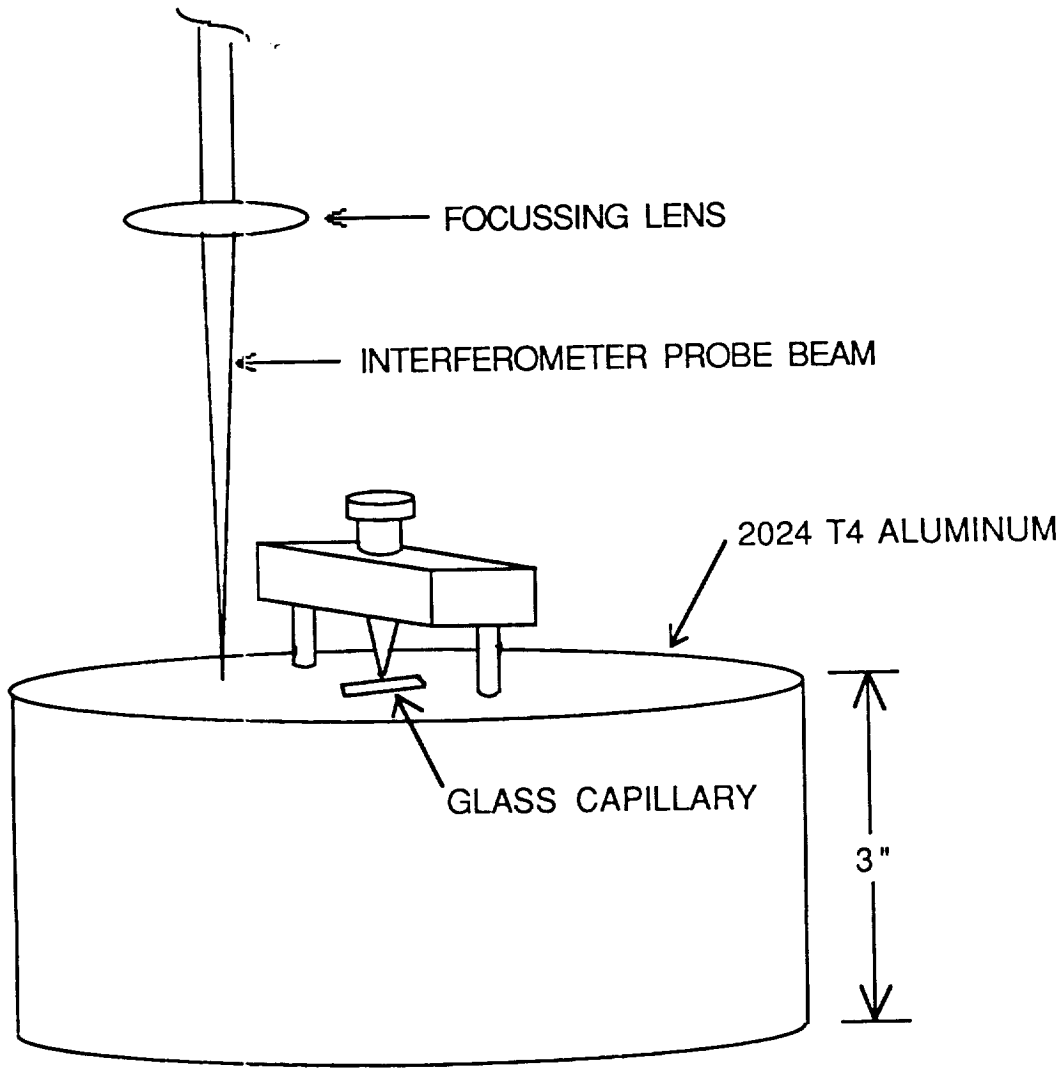

Figure 8. Experimental arrangement for acoustic emission test.

Figure 9 shows the theoretically computed vertical surface displacement versus time record for a step-function time dependence point source load applied to the surface of a homogeneous isotropic linear elastic half-space (129). The longitudinal, shear and Rayleigh surface waves are all indicated. Figure 10 shows the experimentally measured vertical surface displacement versus time record detected with the fiber-optic heterodyne interferometer. The sharp spike characteristic of Rayleigh wave arrival is clearly evident as are the other features predicted theoretically. The second sharp spike is the result of Rayleigh wave reflections from the bounding surfaces of the aluminum test block. The waveform reproduced in Figure 9 has been inverted since the experiment was a step-function time dependence point source unloading one, while the theoretical calculation was performed for the loading case. Since acousto-ultrasonic waves are quite similar to acoustic emission signals, this experiment proved the capability of the fiber-optic heterodyne interferometer to reliably record such waveforms.

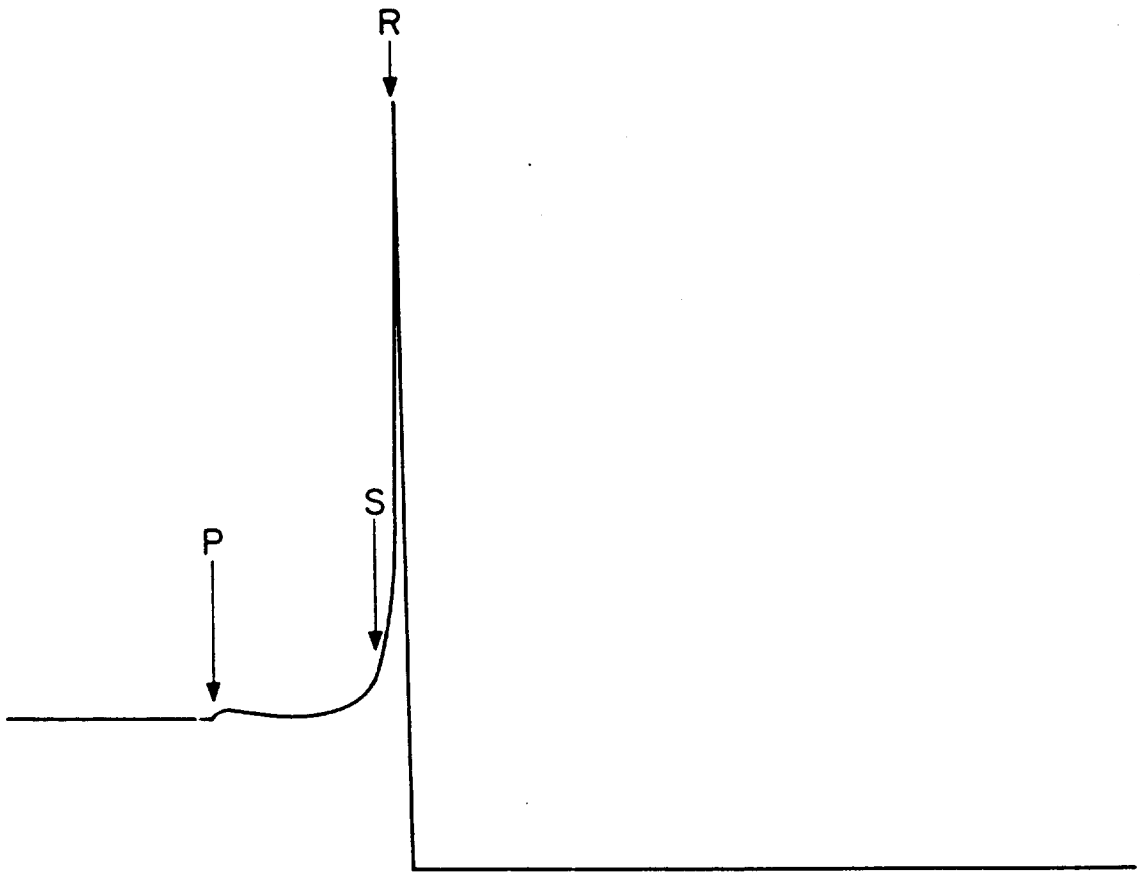

Figure 9. Theoretically predicted vertical surface displacement versus time record for a step-function time dependence point source load applied to the surface of a homogeneous isotropic linear elastic half-space.

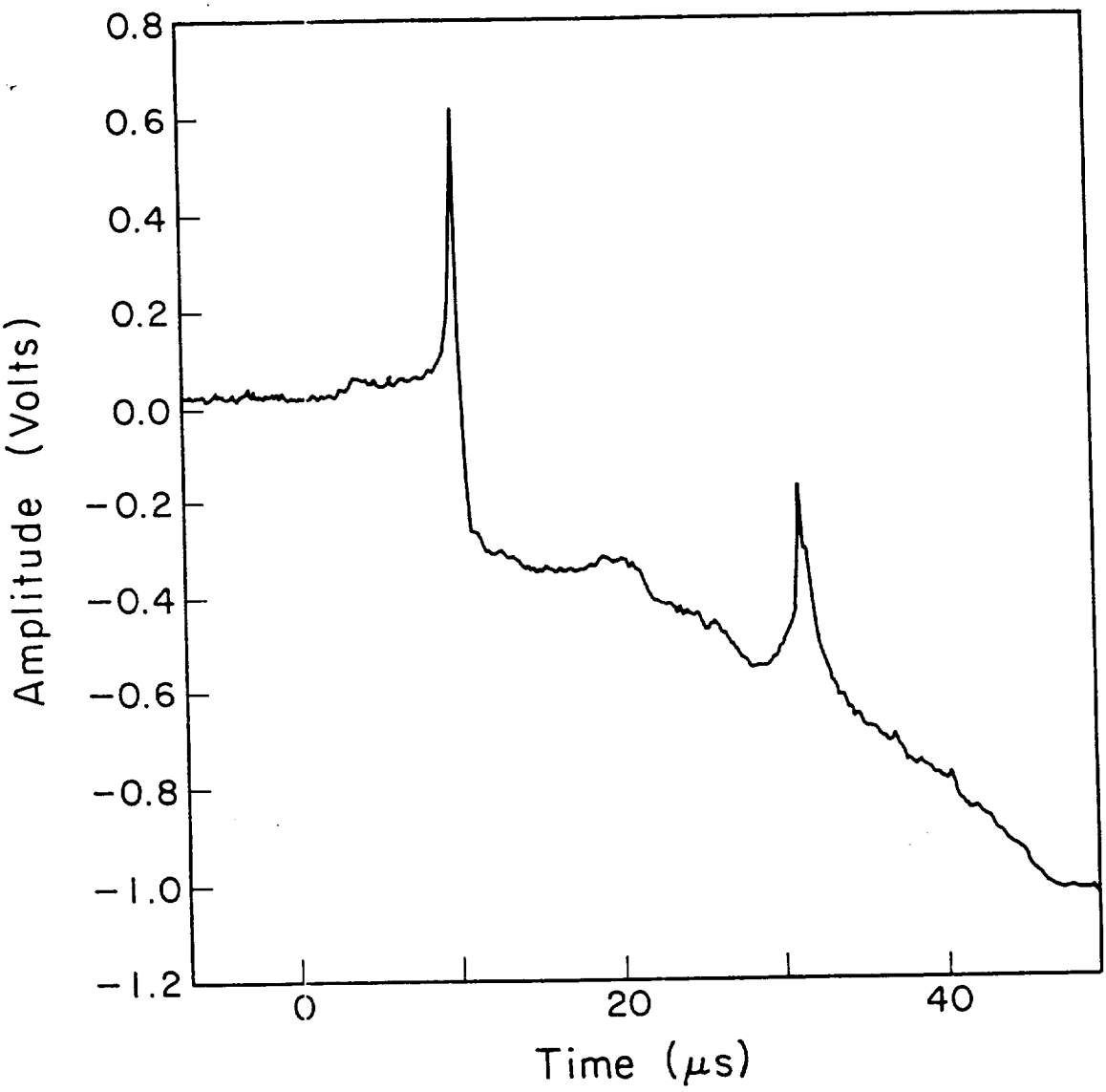

Figure 10. Experimentally measured vertical surface displacement versus time record detected with the fiber-optic heterodyne interferometer.

Detection of Piezoelectric Transducer Generated Ultrasonic Waves

In order to assure that the fiber-optic heterodyne interferometer was capable of detecting the high frequency waves normally encountered in ultrasonic nondestructive evaluation applications tests were run with piezoelectric transducers as ultrasonic wave generators and the fiber-optic heterodyne interferometer as detector. Figure 11 shows the experimental arrangement of one such test to detect ultrasonic pulses generated from a 5MHz piezoelectric transducer coupled to the bottom of a 3 inch thick 2024 T4 aluminum block. Figure 12 shows the ultrasonic waveform detected using the experimental arrangement shown in Figure 11, while Figure 13 shows a longer time record of the same waveform. The Fast Fourier Transform of the 5 MHz piezoelectric generated interferometer detected pulse shown in Figures 12 and 13 is shown in Figure 14. This result clearly shows that the fiber-optic heterodyne interferometer is capable of faithfully detecting MHz frequency waves.

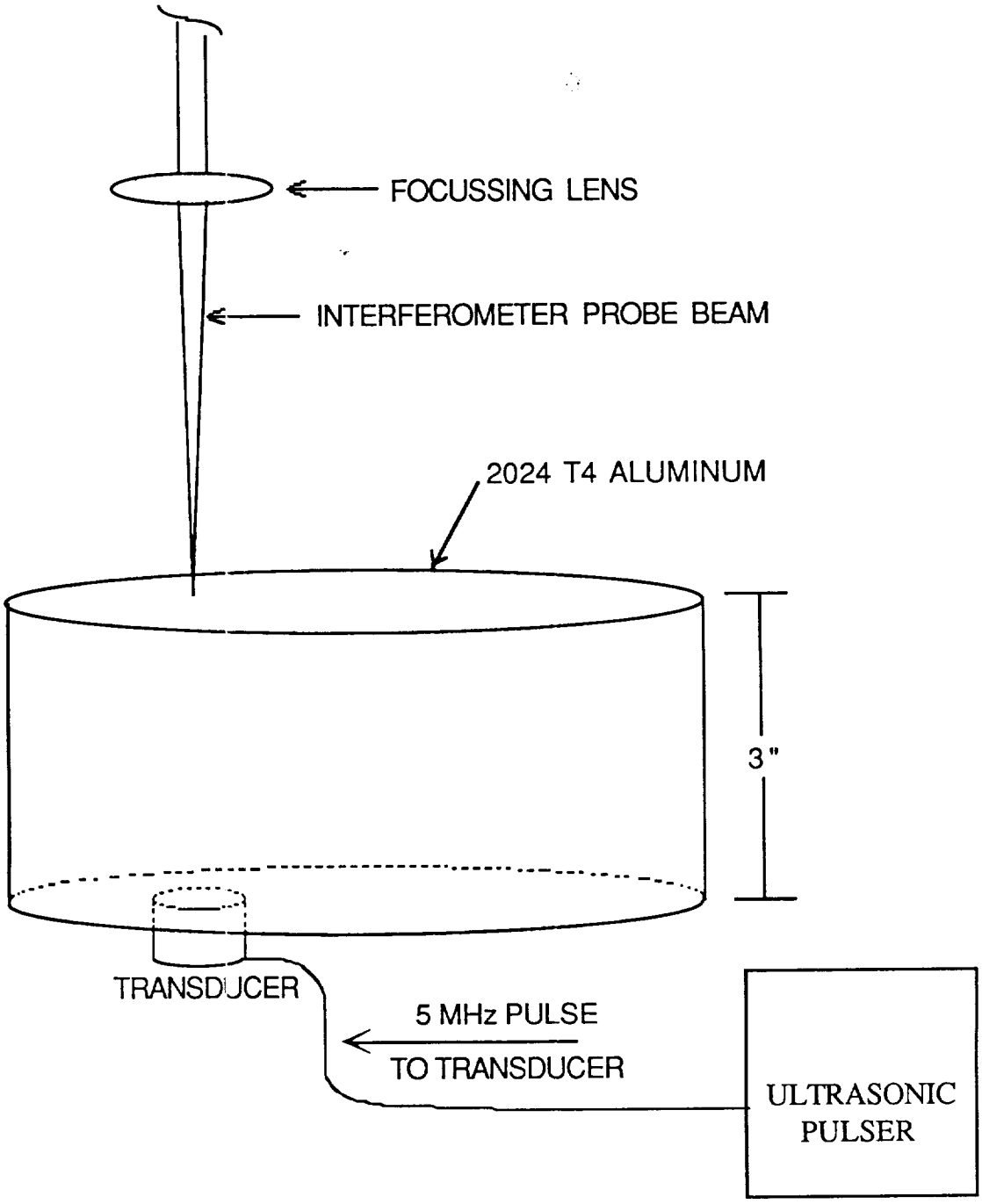

Figure 11. Schematic diagram of experimental arrangement used to detect ultrasonic pulses generated from a 5 MHz piezoelectric transducer coupled to the bottom of a 3 inch thick 2024 T4 aluminum block.

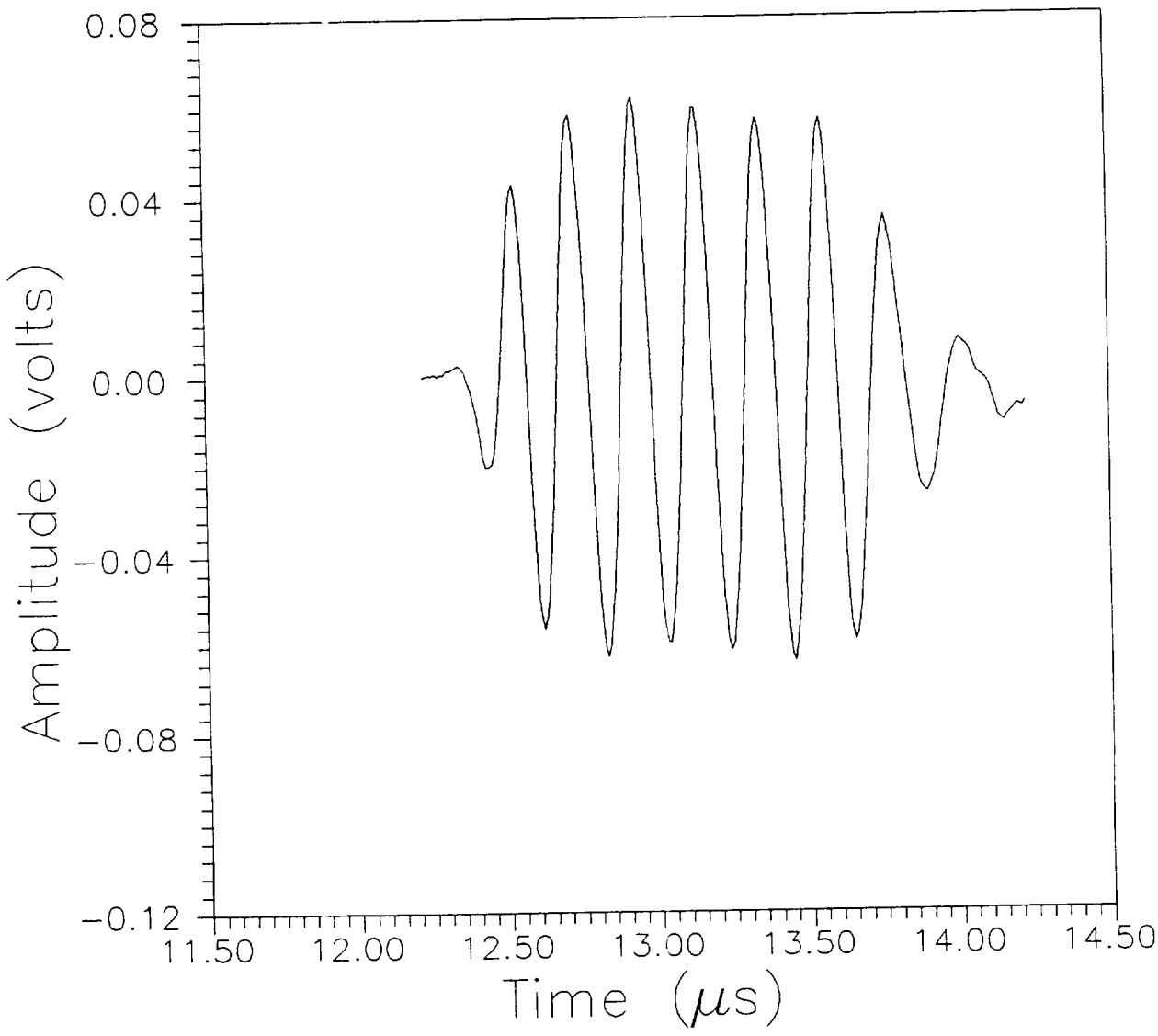

Figure 12. Ultrasonic waveform detected using experimental arrangement shown in Figure 11.

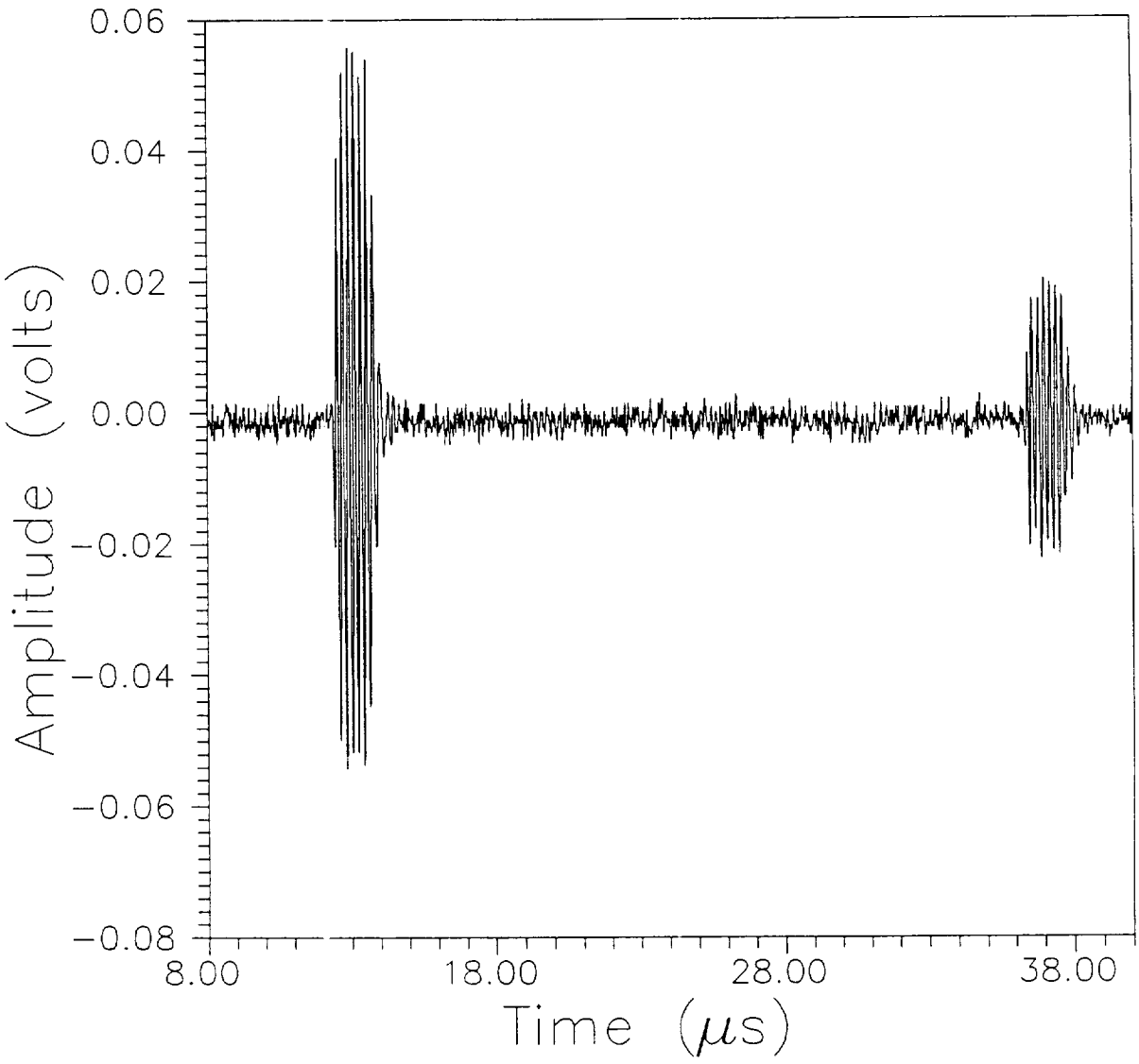

Figure 13. Ultrasonic waveform detected using experimental arrangement shown in Figure 11 (longer time record).

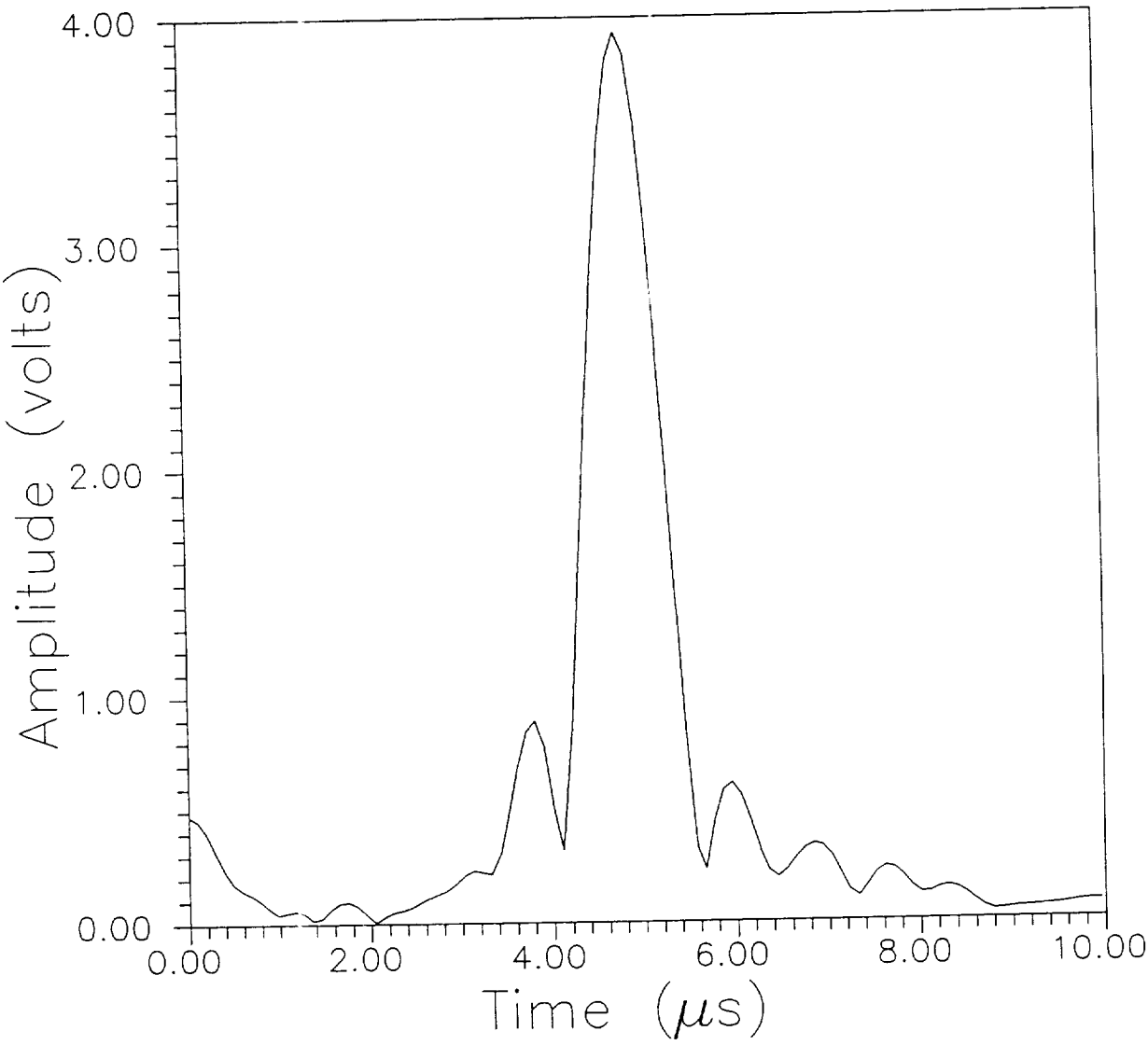

Figure 14. Fast Fourier Transform of 5 MHz ultrasonic pulse obtained using experimental arrangement shown in Figure 11.

Laser Generation/Detection of Ultrasound

The Kigre Nd:YAG pulsed laser was used to generate ultrasonic waves on one side of a 40 mil (1 mm) thick brass plate and the path-stabilized laser interferometer was used to detect the resulting waveforms 1 3/16 in (30mm) away from the epicenter on the other side of the plate. Figure 15 is a schematic of the experimental arrangement used for pulsed laser generation and path-stabilized interferometer detection of ultrasonic waves passing through a brass plate. The test was then repeated using a 2.25 MHz longitudinal mode piezoelectric transducer as the detector for comparison of recorded waveforms with those obtained using the laser interferometer. The piezoelectric transducer was centered at the same position as the interferometer. Figure 16 is the laser interferometer detected waveform and Figure 17 is the piezoelectric transducer detected waveform. The waveform obtained using the interferometer clearly shows the symmetric and asymmetric Lamb modes which are generated in the plate, while the waveform detected with the piezoelectric transducer does not. This clearly shows that the laser interferometer is capable of detecting a broad band of ultrasonic frequencies. Moreover, since the detection is constant over the frequency band, the output is an accurate record of the specimen surface displacement.

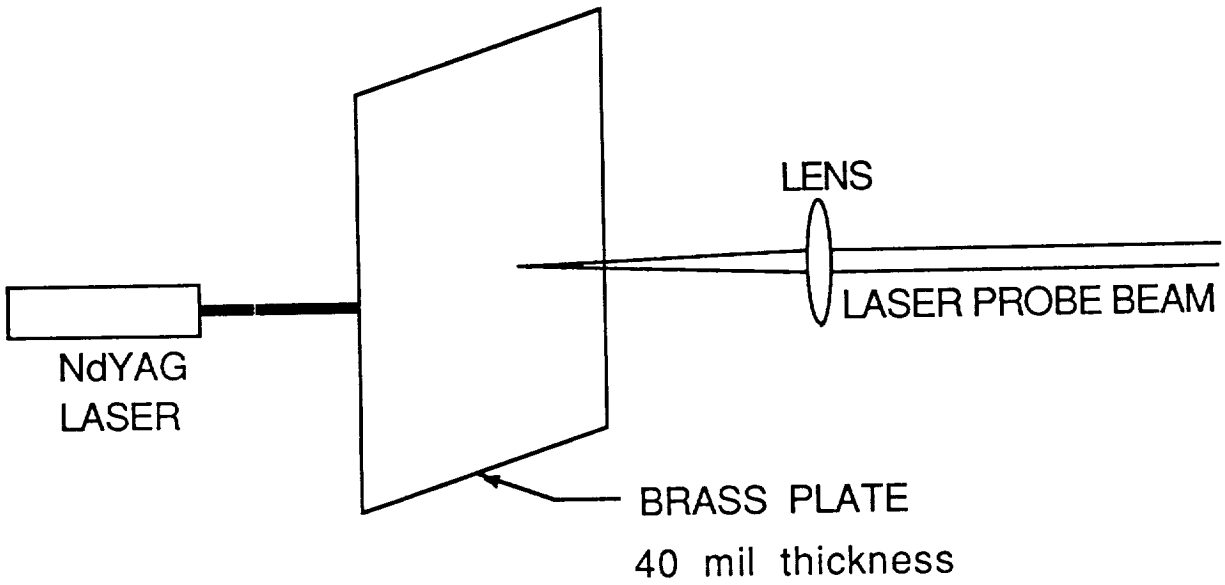

Figure 15. Schematic of experimental arrangement for pulsed laser generation and path stabilized interferometer detection of ultrasonic waves passing through a brass plate.

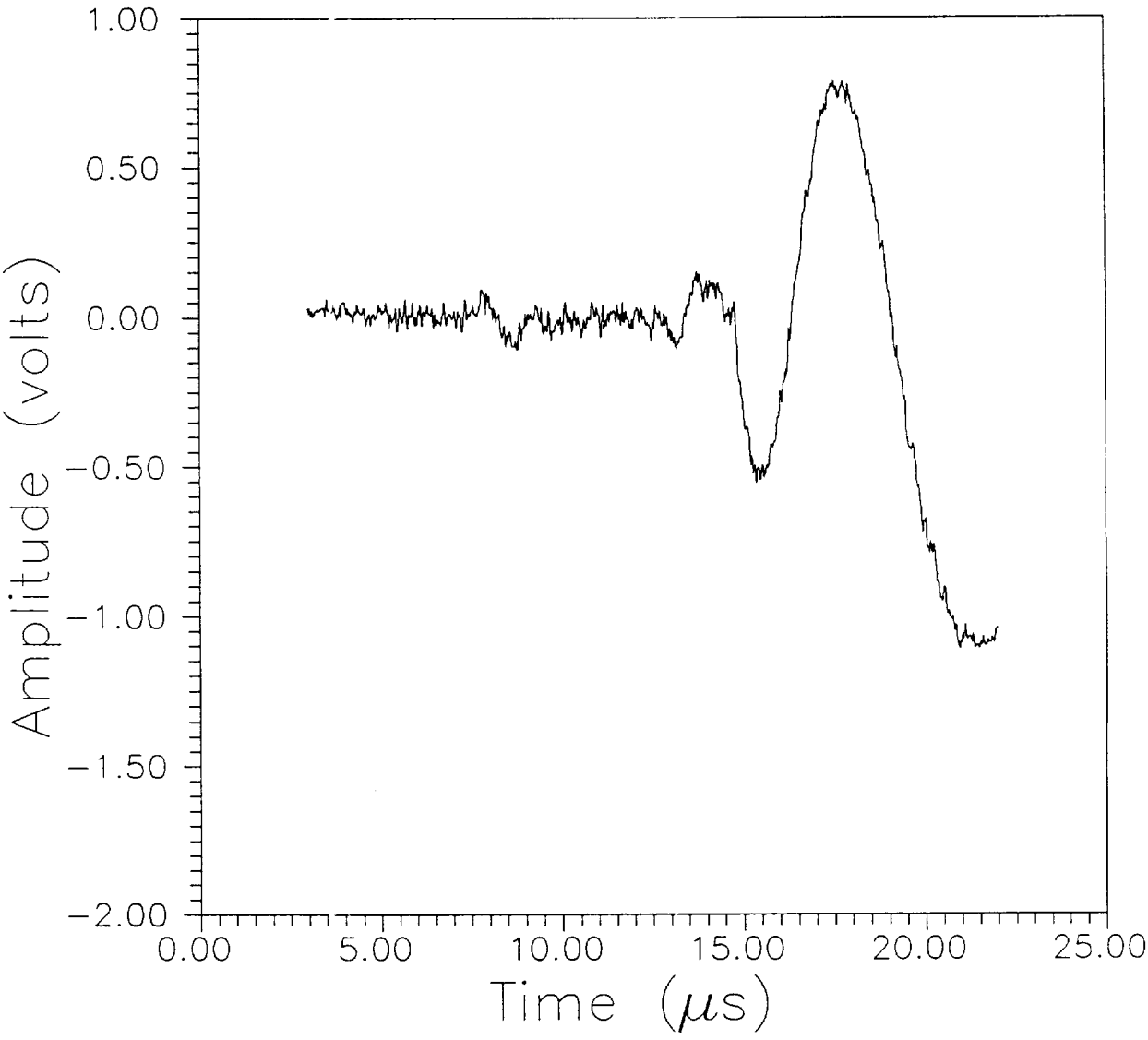

Figure 16. Pulsed laser generated path-stabilized laser interferometer detected waveform of ultrasonic wave passing through brass plate.

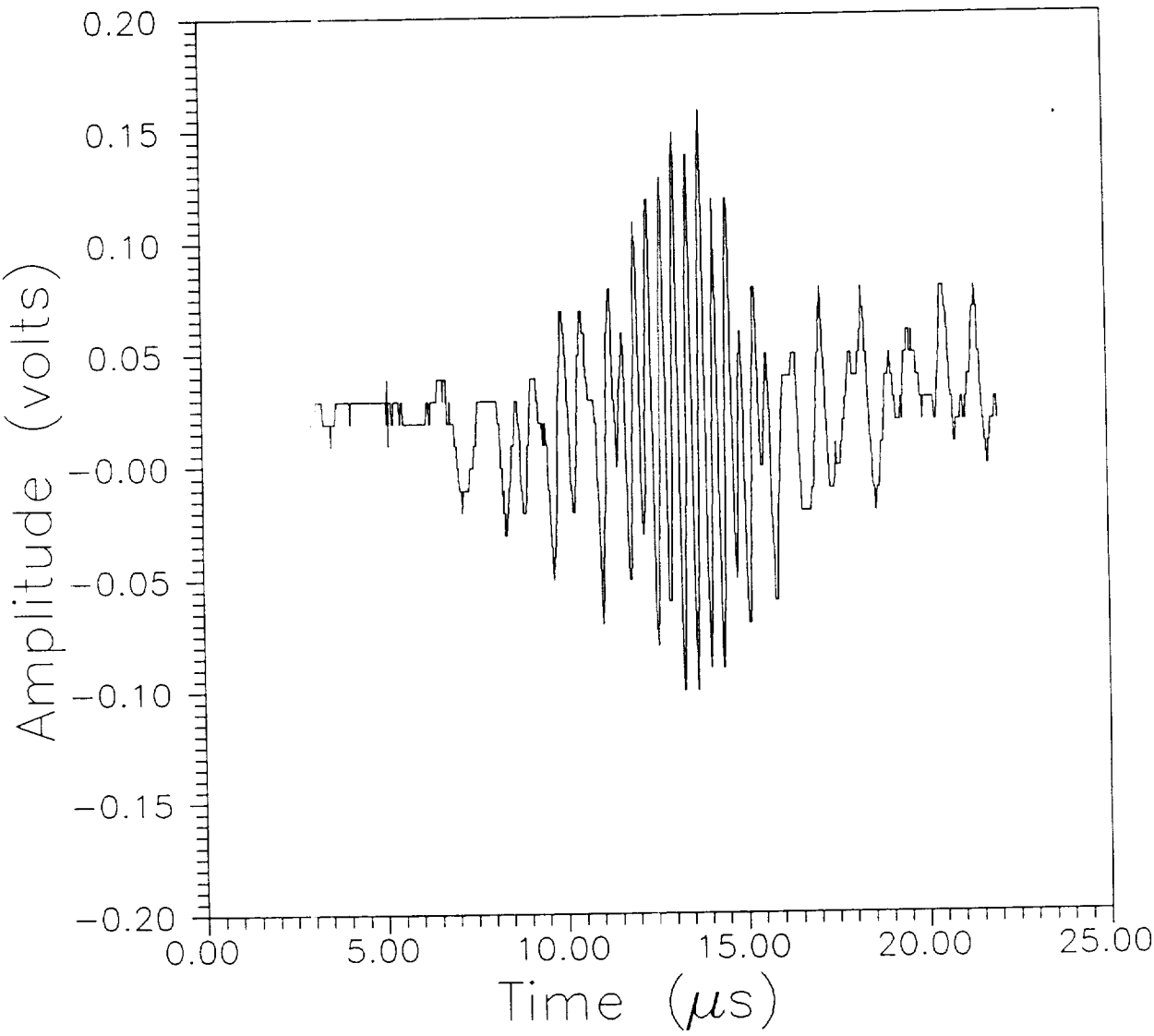

Figure 17. Pulsed laser generated piezoelectric transducer detected waveform of ultrasonic wave passing through same brass plate as in Figure 16.

Additional experiments were conducted using the Kigre Nd:YAG pulsed laser to generate ultrasonic waves on one face of a 1.5 in (38 mm) thick block of aluminum. The displacement on the opposite face due to the propagating ultrasonic wave was detected using the path-stabilized laser interferometer. Figure 18 is a schematic of the experimental arrangement for this test. The test was then repeated using a 2.25 MHz longitudinal wave piezoelectric transducer as a detector for comparison purposes. For these tests two detection sites were used. One site was on epicenter and the other was off epicenter: both detection sites on the face opposite the generation one. A thin coating of black marker ink was put on the surface of the aluminum block at the generation site in order to increase the amplitude of the ultrasonic wave. The Nd:YAG laser pulse caused the marker coating to ablate which led to an increase in the amplitude of the ultrasound at the detection sites.

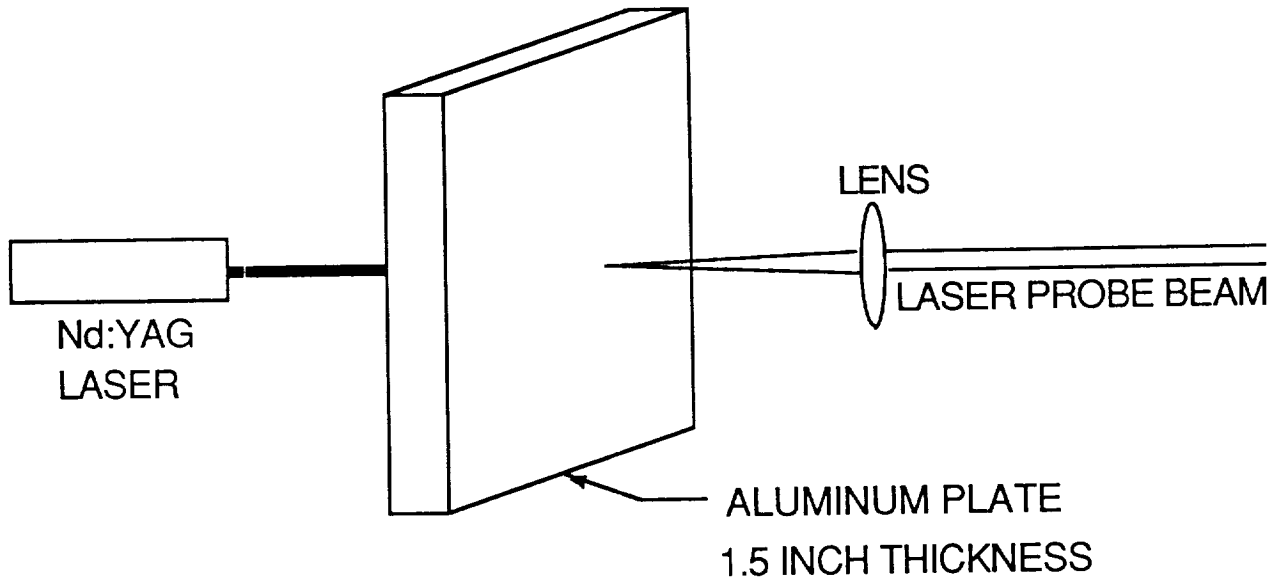

Figure 18. Schematic of experimental arrangement for pulsed laser generation and path-stabilized interferometer detection of ultrasonic waves passing through an aluminum block

Calculations for the theoretical surface displacement on the detecting face of the aluminum block due to the impingement of the Nd:YAG laser pulse on the opposite side were made using a computer program supplied by Hsu (130). This program was modified to convolve the resultant detected waveform with the laser pulse in order to yield a surface displacement which was more representative of the actual test conditions. Figure 19 shows the theoretical surface displacement for the pulsed laser generated ultrasound in the aluminum block detected on epicenter. Figure 20 shows the actual waveform detected by the path-stabilized interferometer on epicenter. Excellent agreement with the theoretically computed surface displacement was obtained with the interferometer. The longitudinal, shear and reflected longitudinal waves were all correctly detected. Figure 21 shows the waveform obtained using a 2.25 MHz longitudinal wave piezoelectric transducer to detect the laser generated ultrasound on epicenter. Although the transducer was able to detect the longitudinal arrival, it rang upon arrival of the longitudinal waves and the ramping of the surface after the first longitudinal spike resulting from the shear wave was not detected.

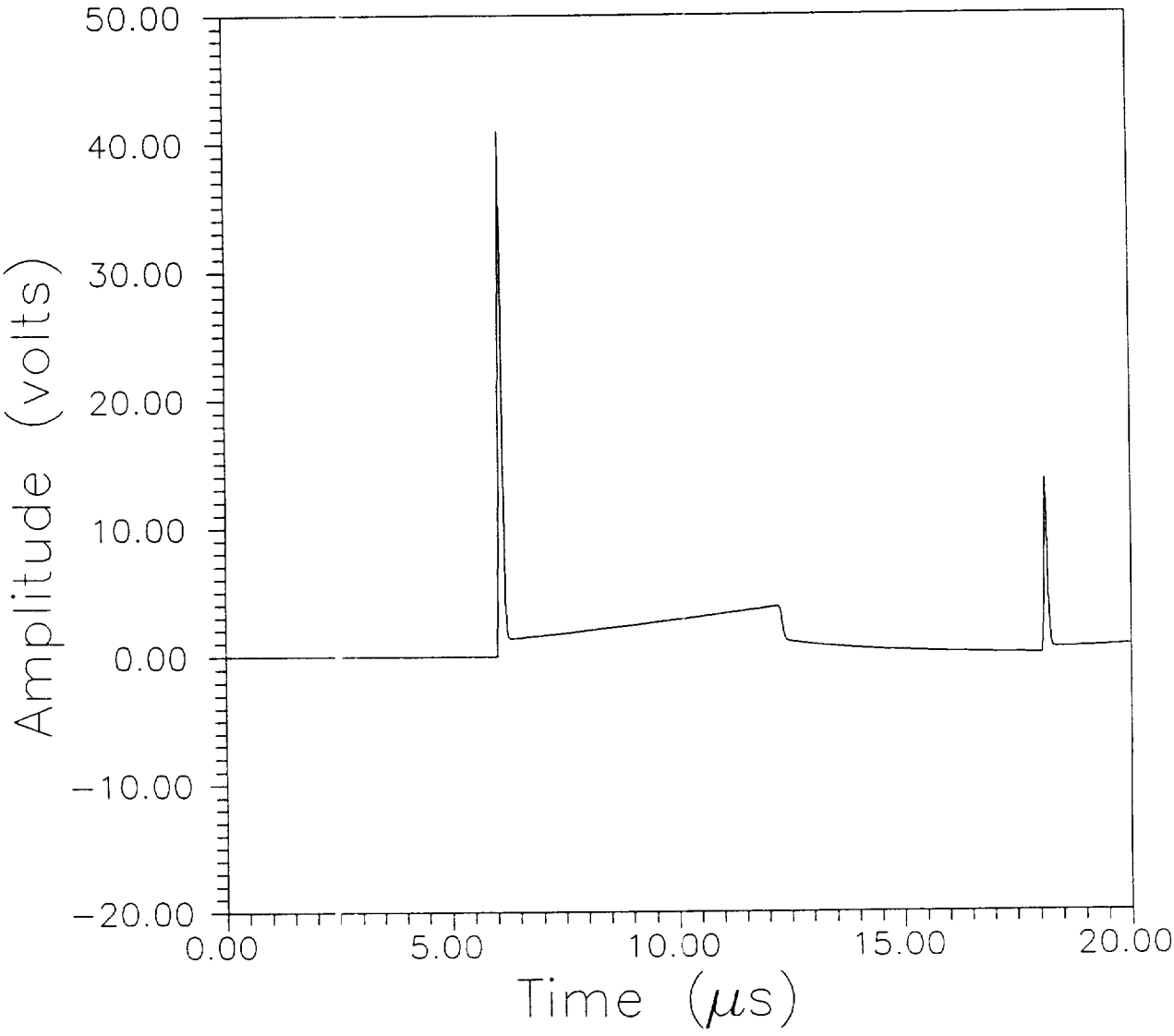

Figure 19. Theoretical surface displacement for pulsed laser generated ultrasound in aluminum block detected on epicenter.

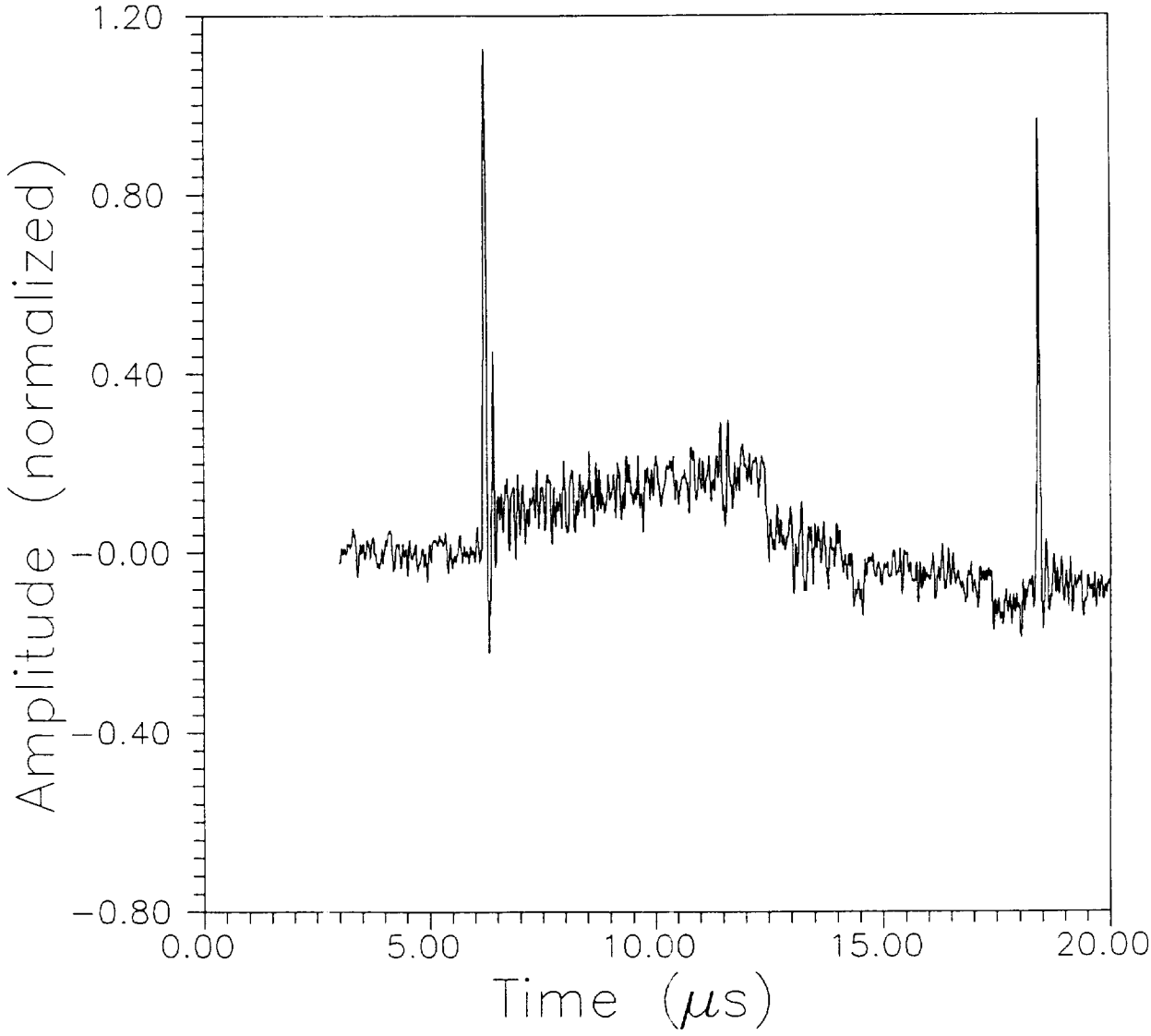

Figure 20. Surface displacement for pulsed laser generated ultrasound in aluminum block detected by path-stabilized interferometer on epicenter.

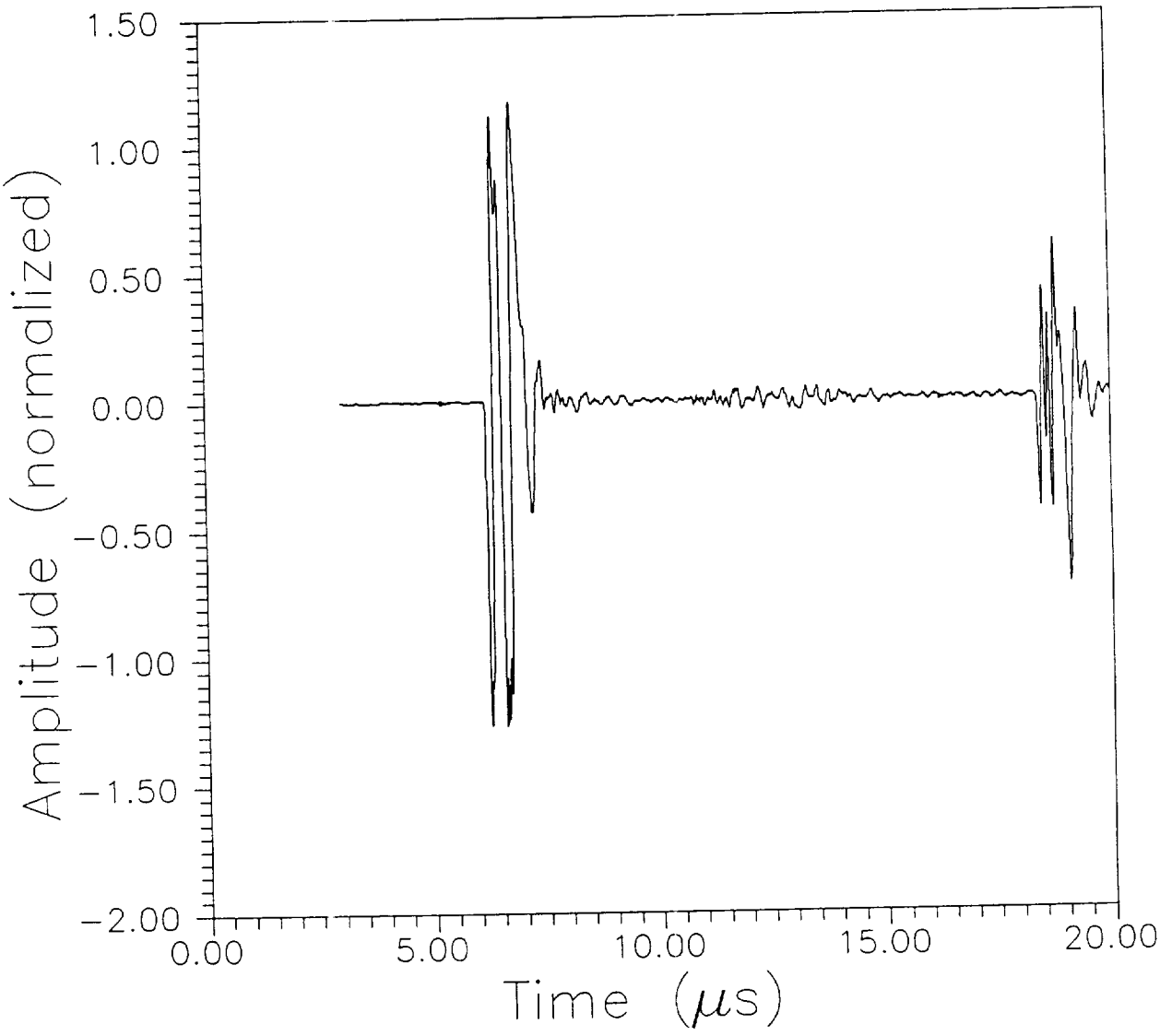

Figure 21. Waveform obtained for pulsed laser generated ultrasound in aluminum block detected by 2.25 MHz piezoelectric transducer on epicenter.

Figure 22 shows the theoretical surface displacement 7/8 in (22 mm) off epicenter due to pulsed laser generation on the opposite surface of the 1.5 in (38mm) aluminum block. Figure 23 shows the waveform obtained at the 7/8 in (22 mm) off epicenter position using the path-stabilized laser interferometer. Once again, excellent agreement with the theoretical predicted surface displacement is observed, as the longitudinal mode converted head and reflected longitudinal waves are clearly detected. Figure 24 shows the waveform obtained at the same position using the 2.25 MHz longitudinal wave piezoelectric transducer. As with the test on epicenter, it is quite clear that the piezoelectric transducer does not give an accurate record of the displacement of the surface of the material resulting from the laser pulse incident on the opposite side of the block. There is ringing in the piezoelectric transducer upon arrival of the longitudinal waves. In addition, the piezoelectric transducer record does not show the ramping of the surface and does not pick up the mode converted head wave properly.

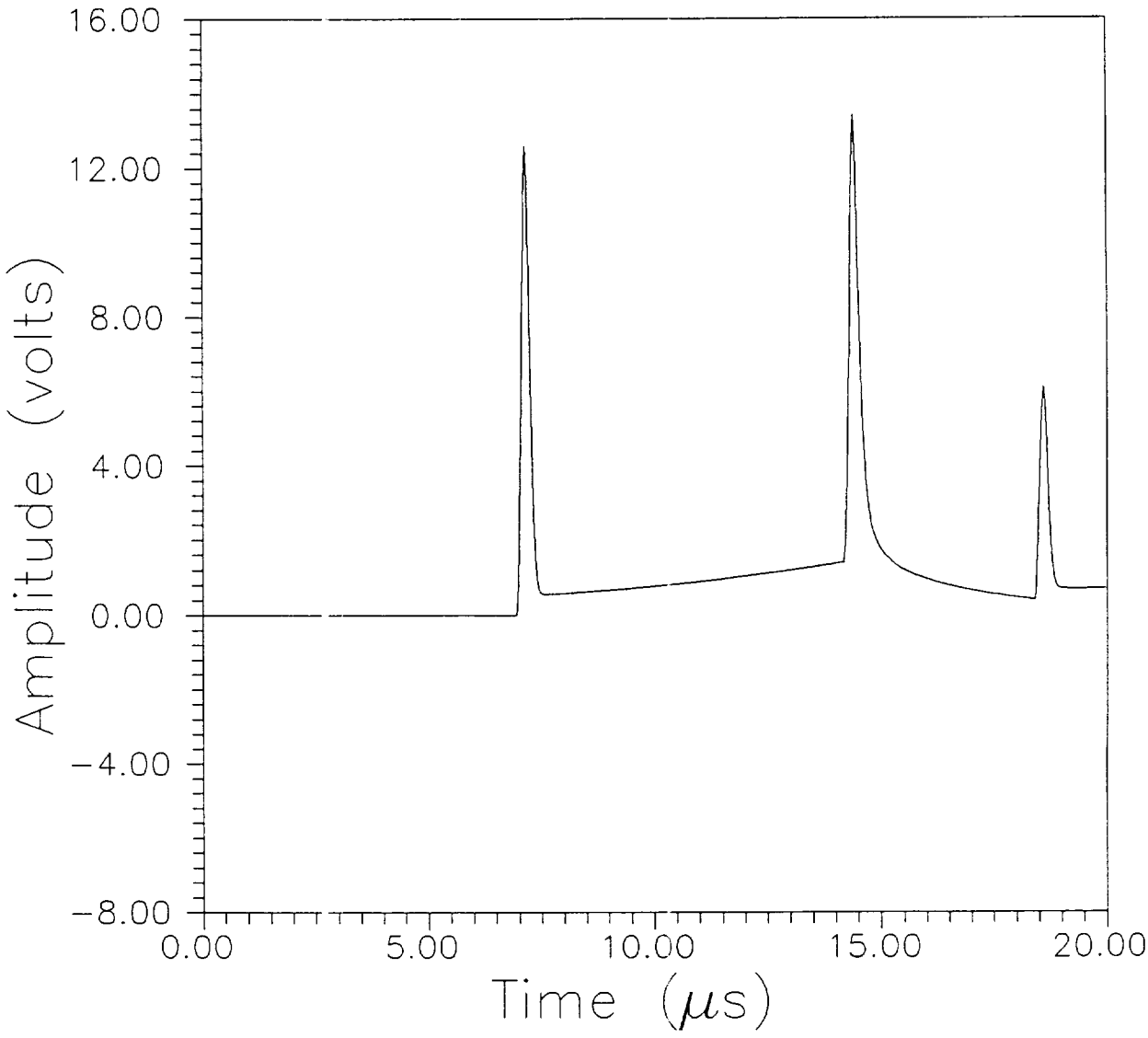

Figure 22. Theoretical surface displacement for pulsed laser generated ultrasound in aluminum block detected 7/8 in (22 mm) off epicenter.

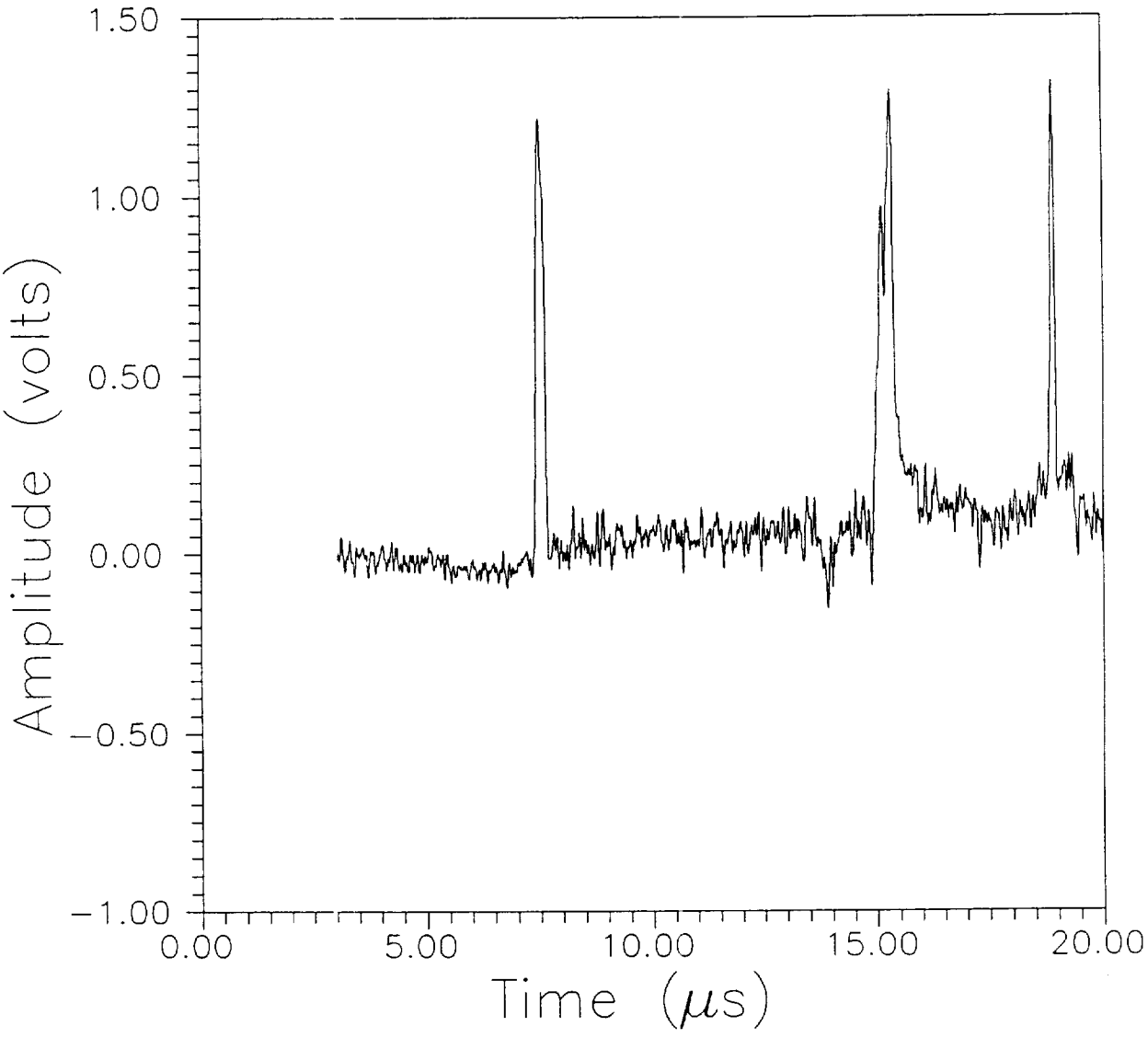

Figure 23. Surface displacement for pulsed laser generated ultrasound in aluminum block detected by path-stabilized interferometer at the 7/8 in (22 mm) off epicenter position.

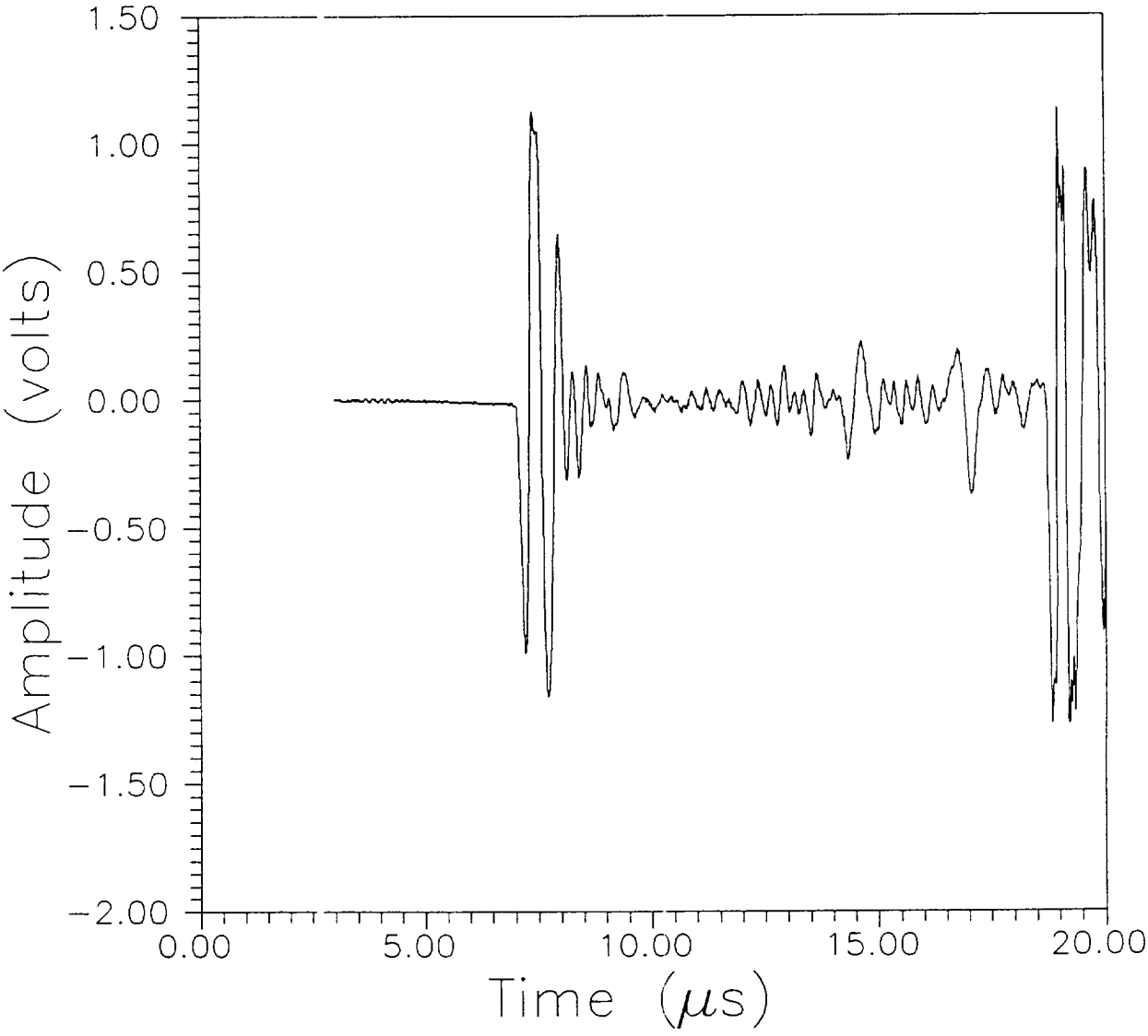

Figure 24. Waveform obtained for pulsed laser generated ultrasound in aluminum block detected by 2.25 MHz piezoelectric transducer at the 7/8 in (22 mm) off epicenter position.

Laser Acousto-Ultrasonics

A series of experiments were conducted to compare acousto-ultrasonic waveforms generated and detected by a commercial AET 206 AU instrument, with the waveforms generated by the pulsed laser and detected with a conical point piezoelectric transducer, and with the waveforms generated by the pulsed laser and detected with the fiber-optic heterodyne interferometer. The laser interferometer was used to detect the surface displacements and then the conical point piezoelectric transducer was used to detect the displacements at the same point. In both cases, the generating laser pulse was incident on the same spot on the specimens and the transducer was placed at the same location as the interferometer probe beam in order to keep the source to detector distances at two inches. Figure 25 is a diagram showing the geometrical arrangement for these tests; the source to detector distance was 2 in (50 mm). In keeping with the design of the commercial acousto-ultrasonic instrument, generation and detection of the ultrasonic waveforms was conducted on the same side of the specimens. The Kigre Nd:YAG pulsed laser was used to generate ultrasound in the thermoelastic regime in several composites samples. Either the fiber-optic heterodyne laser interferometer or the conical point piezoelectric transducer was used to detect the resulting surface displacements. The conical point piezoelectric transducer was used because previous work had shown that it was capable of faithfully reproducing the theoretically predicted acoustic emission waveforms over a fairly broad band of frequencies.

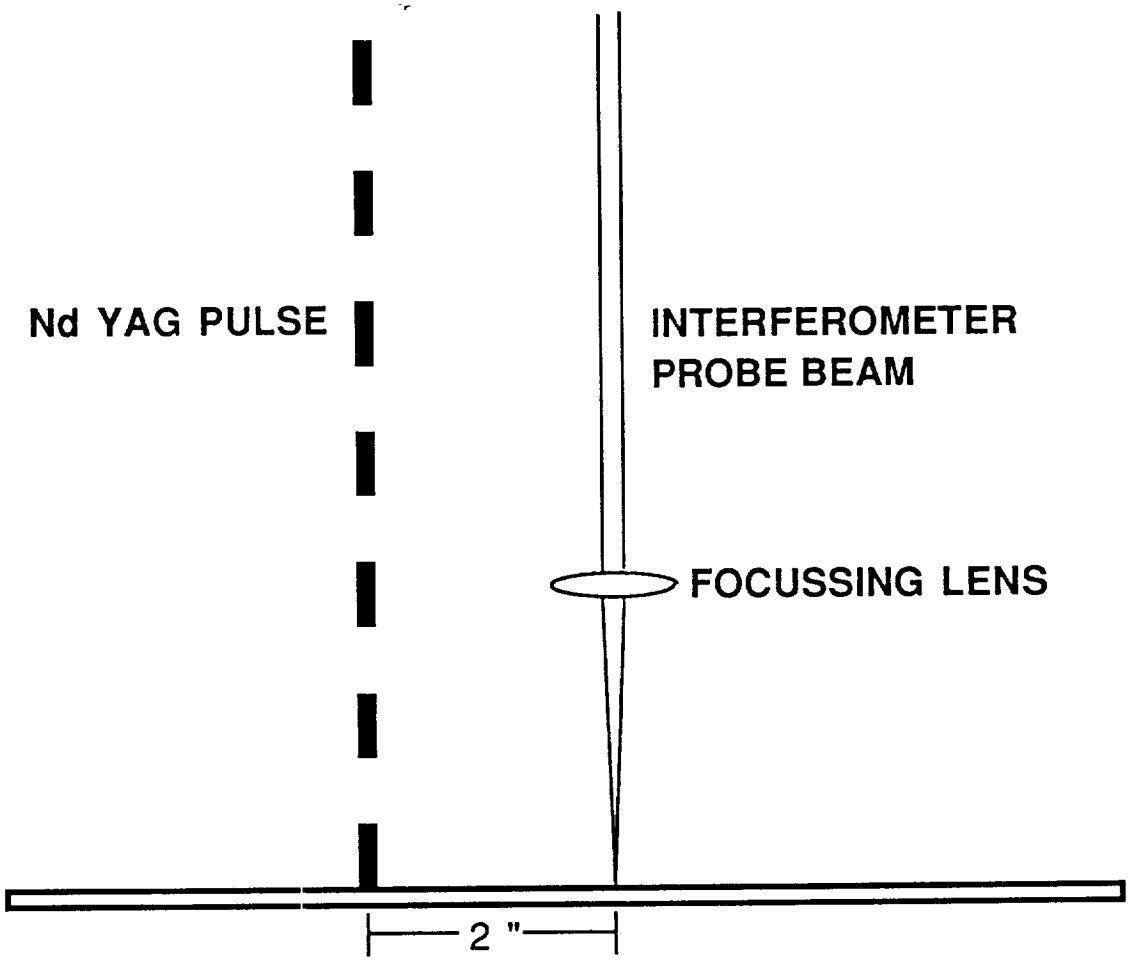

Figure 25. Diagram showing the geometrical arrangement for acousto-ultrasonic tests

Three different composite specimens provided by the NASA Lewis Research Center were tested: a graphite/epoxy 90 degree laminate, a graphite/epoxy cross-ply, and a filament wound composite. The geometrical shape and dimensions of these specimens are shown in Figure 26. In order to increase the reflectivity at the point of detection on the black specimens, 3M silver polyester film tape was stuck to the specimens at the detection sites. The silver tape was also left on the specimens when the conical point piezoelectric transducer detector was used in order to maintain the same test conditions for the two detectors. The silver tape serves to increase the reflectivity of specimens and thereby increase the detection sensitivity of optical interferometers when probing poorly reflecting material surfaces.

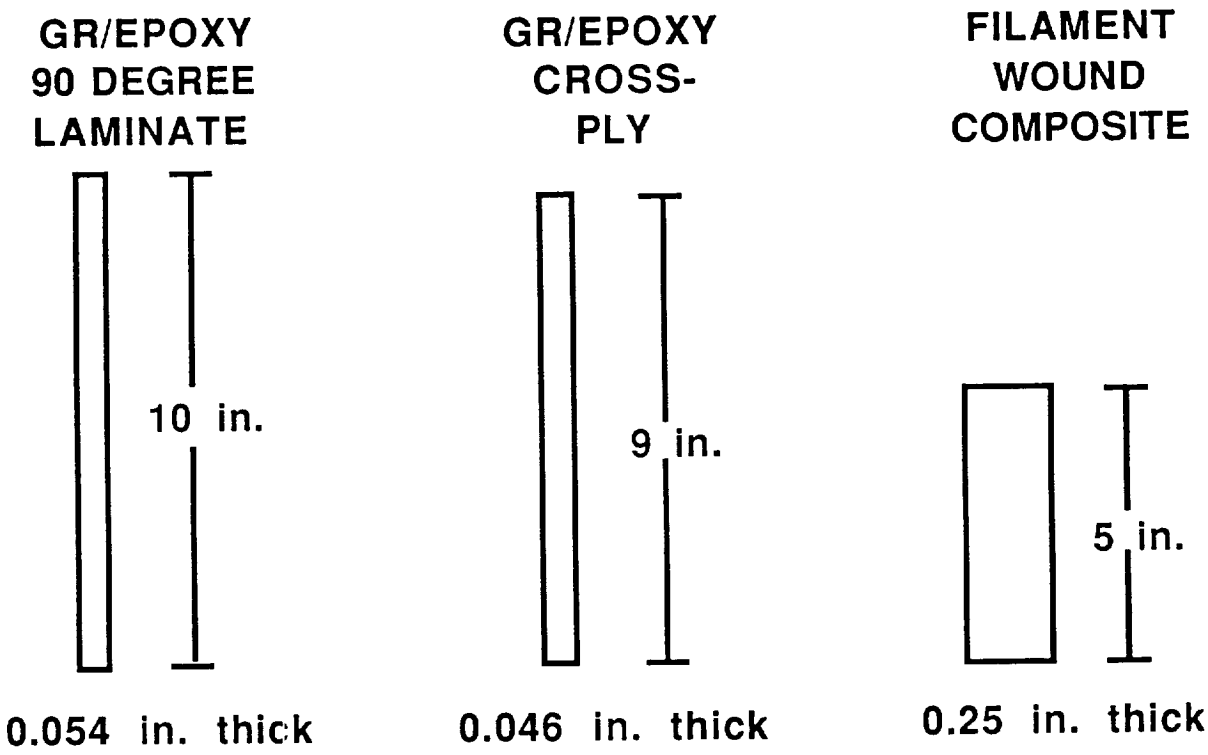

Figure 26. Geometric shape and dimensions of acousto-ultrasonic specimens

Figure 27 shows the pulsed laser generated fiber-optic heterodyne laser interferometer detected waveform for the graphite/epoxy 90 degree laminate specimen. Figure 28 shows the conical point piezoelectric transducer detected waveform for the same specimen. This specimen was quite thin (0.054 in, 1.1 mm) and, as is well known, the geometry of the specimen plays a major role in the type of waves which will propagate through it. The interferometer detected waveform shows that an asymmetric mode Lamb wave was generated in this specimen. However, the piezoelectric transducer detected waveform does not show that a plate wave is propagating through this thin material.

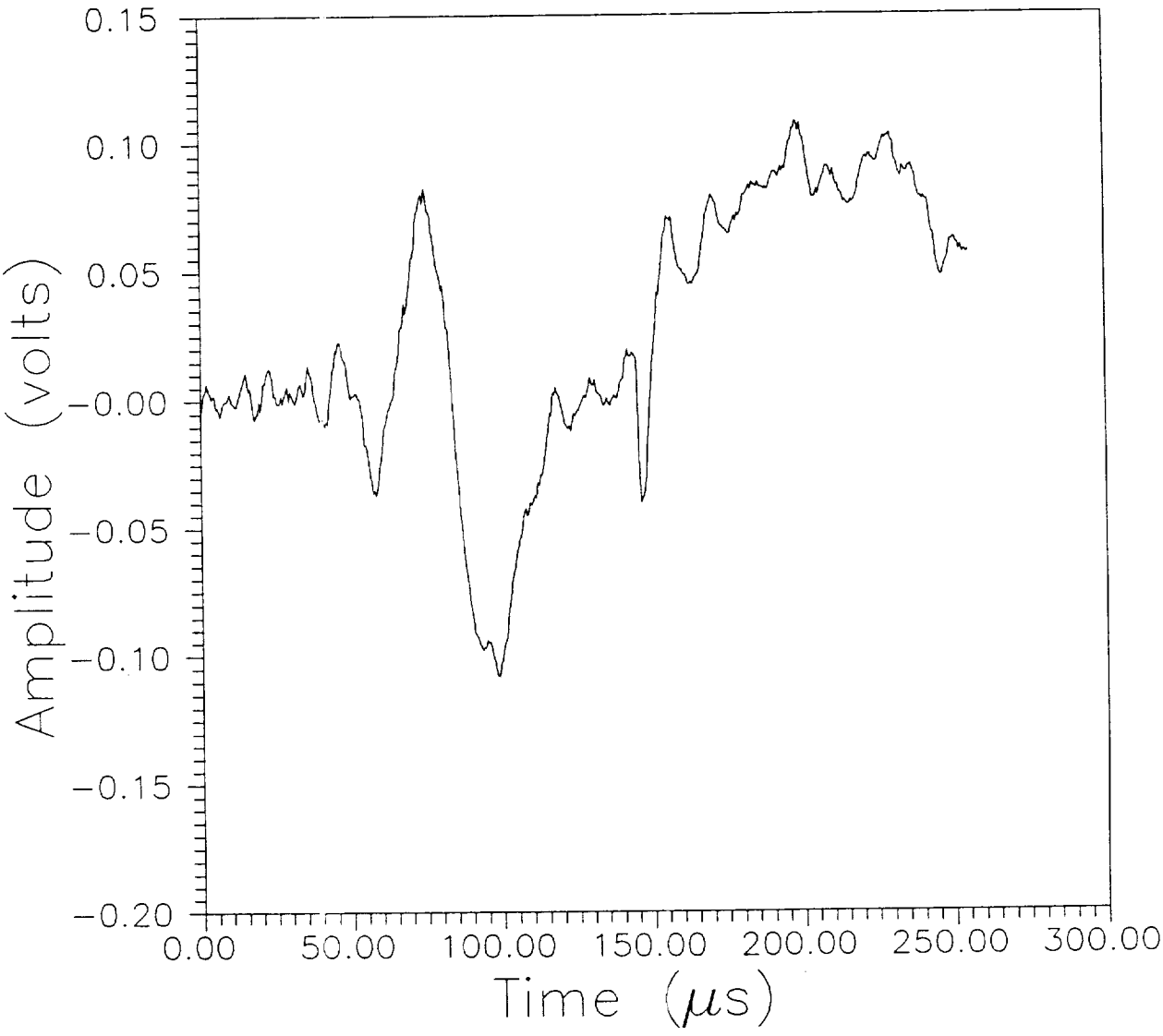

Figure 27. Pulsed laser generated fiber-optic heterodyne laser interferometer detected waveform for the graphite/epoxy 90 degree laminate specimen.

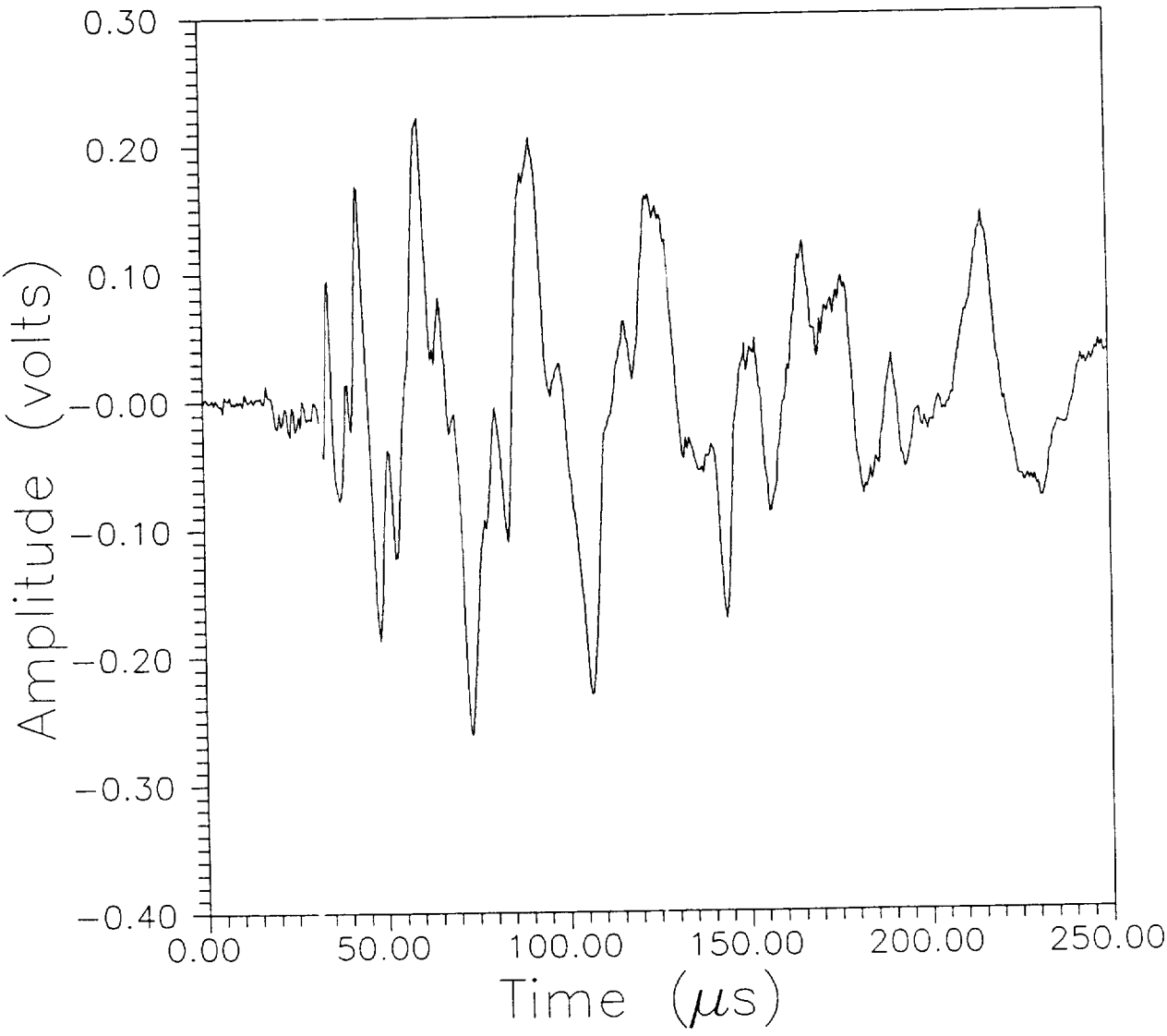

Figure 28. Pulsed laser generated conical point piezoelectric transducer detected waveform for the graphite/epoxy 90 degree laminate specimen.

The pulsed laser generated fiber-optic heterodyne laser interferometer detected waveform for the graphite/epoxy cross-ply laminate specimen is shown in Figure 29, while the waveform for the same experimental situation as detected with the point conical piezoelectric transducer is shown in Figure 30. As with the graphite/epoxy 90 degree laminate, the cross-ply sample was quite thin (0.046 in, 1 mm) and once again plate waves were generated in the specimen by the pulsed laser. Again, the interferometer faithfully detected the asymmetric Lamb mode wave which propagated through the specimen, but the piezoelectric transducer did not.

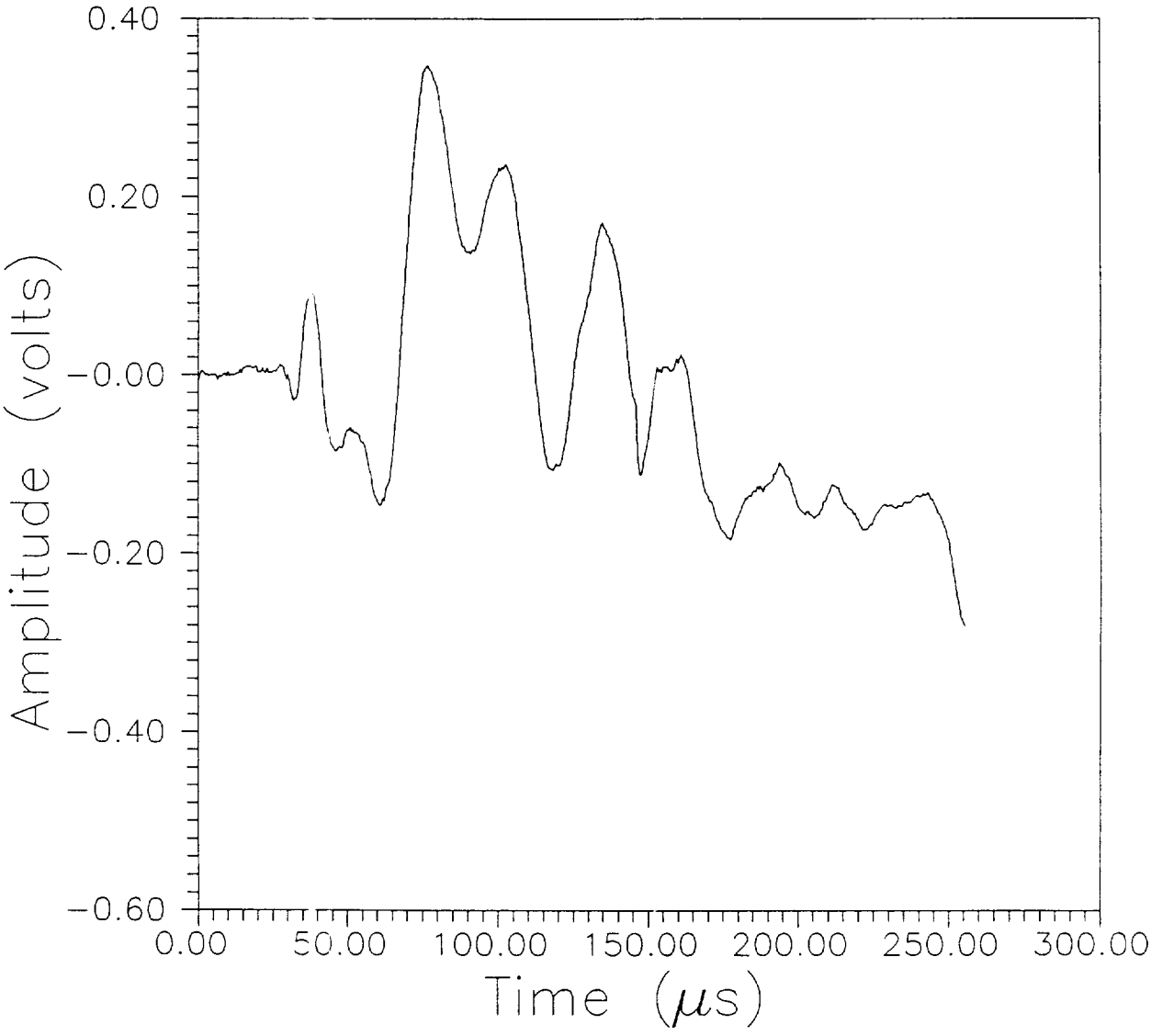

Figure 29. Pulsed laser generated fiber-optic heterodyne laser interferometer detected waveform for the graphite/epoxy cross-ply laminate specimen.

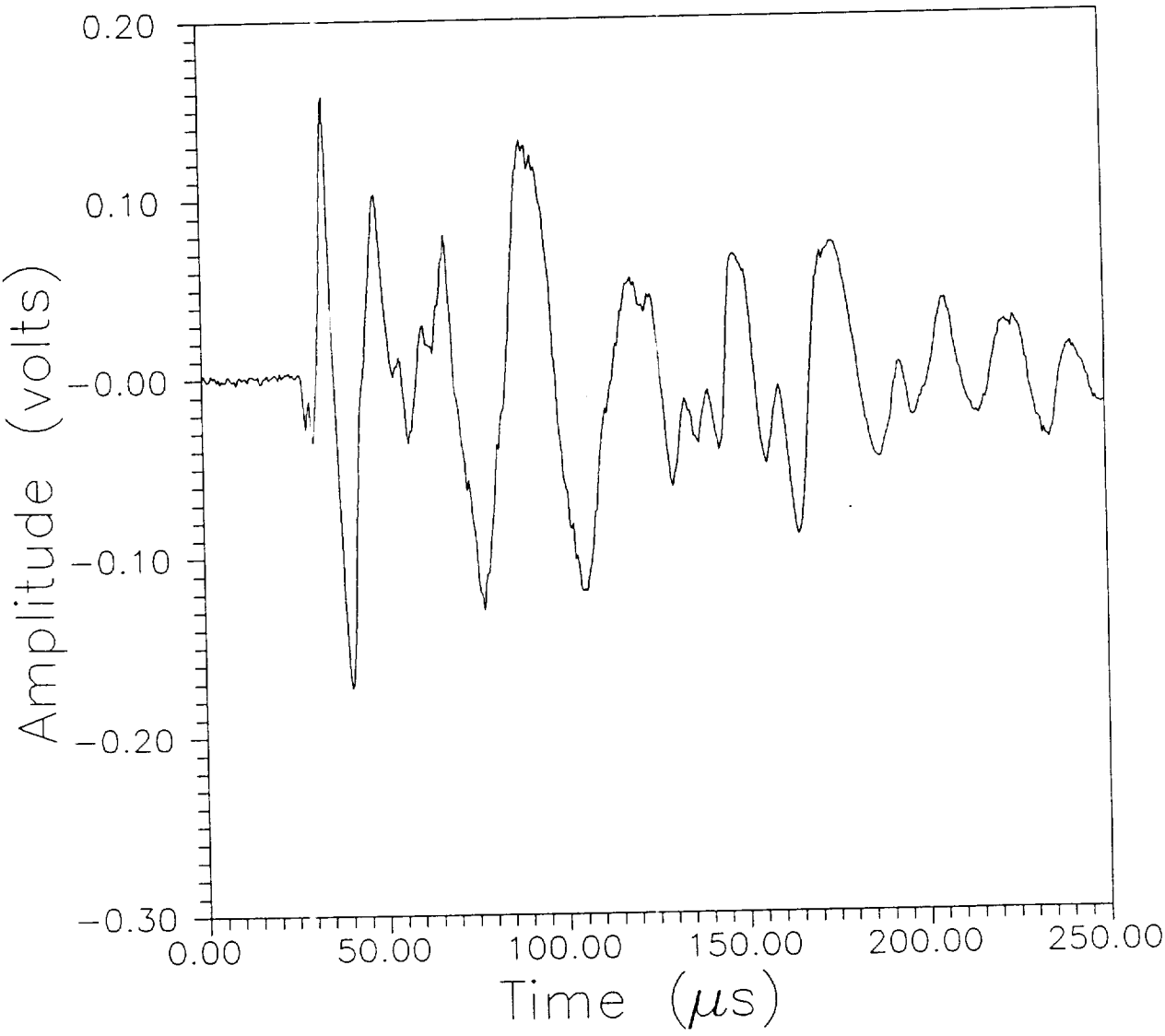

Figure 30. Pulsed laser generated conical point piezoelectric transducer detected waveform for the graphite/epoxy crosss-ply laminate specimen.

Figure 31 shows the pulsed laser generated fiber-optic heterodyne laser interferometer detected waveform for the filament wound composite specimen, while Figure 32 shows the conical point piezoelectric transducer detected waveform for the same specimen. Since this specimen was much thicker than the other two, bulk waves were generated. The two waveforms recorded from this specimen are similar showing that for this specimen geometry the broad band point conical piezoelectric transducer and the fiber-optic heterodyne interferometer are both capable of detecting bulk waves propagating through the specimen.

On the interferometer detected waveforms, an air blast wave from the Nd:YAG laser pulse occurs at approximately 150 microseconds. A similar blast wave was also captured by the interferometer on the other two waveforms.

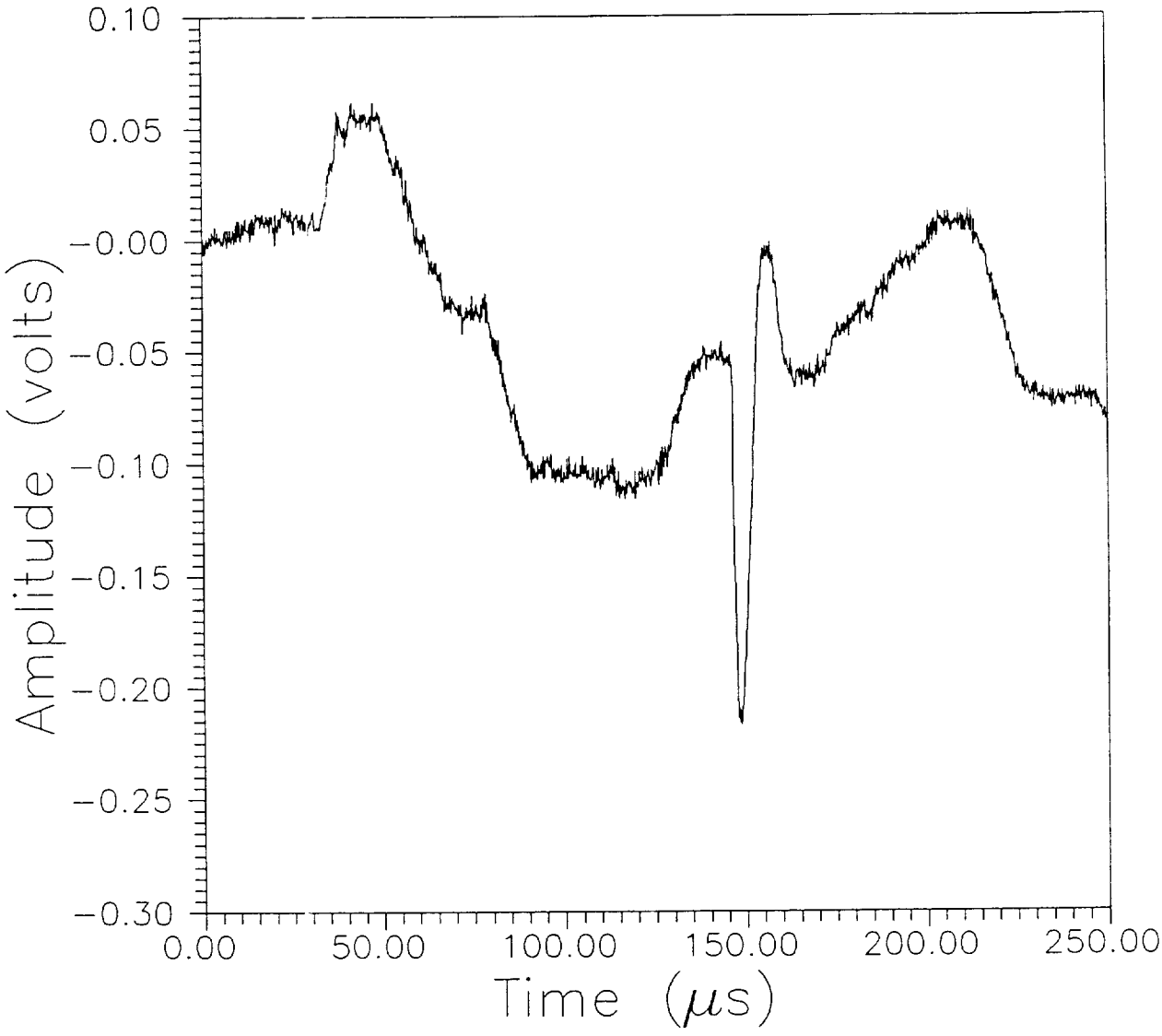

Figure 31. Pulsed laser generated fiber-optic heterodyne laser interferometer detected waveform for the filament wound composite specimen.

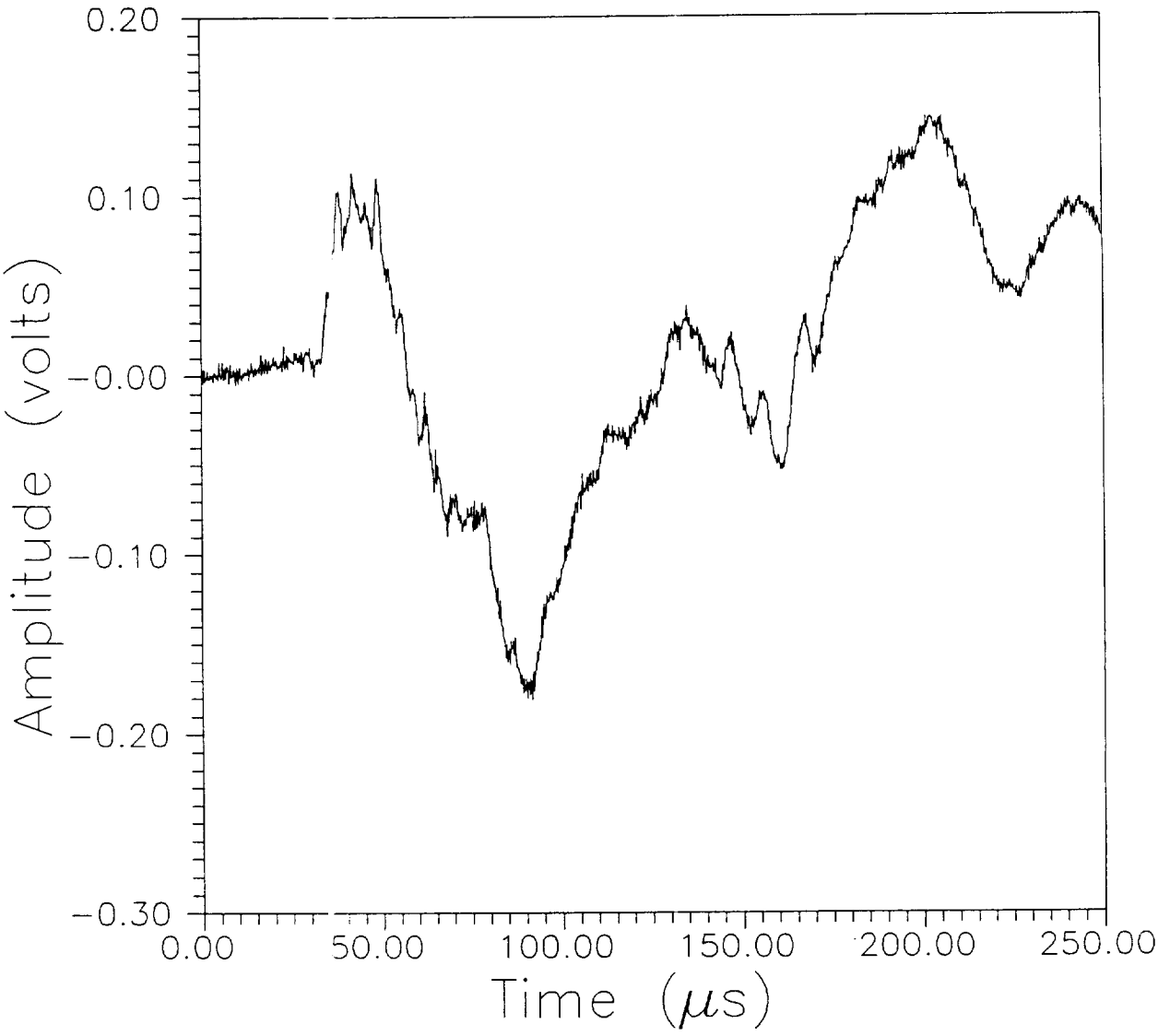

Figure 32. Pulsed laser generated conical point piezoelectric transducer detected waveform for the filament wound composite specimen.

For comparison purposes, an AET 206 AU unit was used to run acousto-ultrasonic tests on the same three composite specimens. Figures 33-35 show the waveforms using the AET 206 AU unit for the graphite/epoxy 90 degree laminate, the graphite/epoxy cross-ply laminate, and the filament wound composite specimens, respectively.

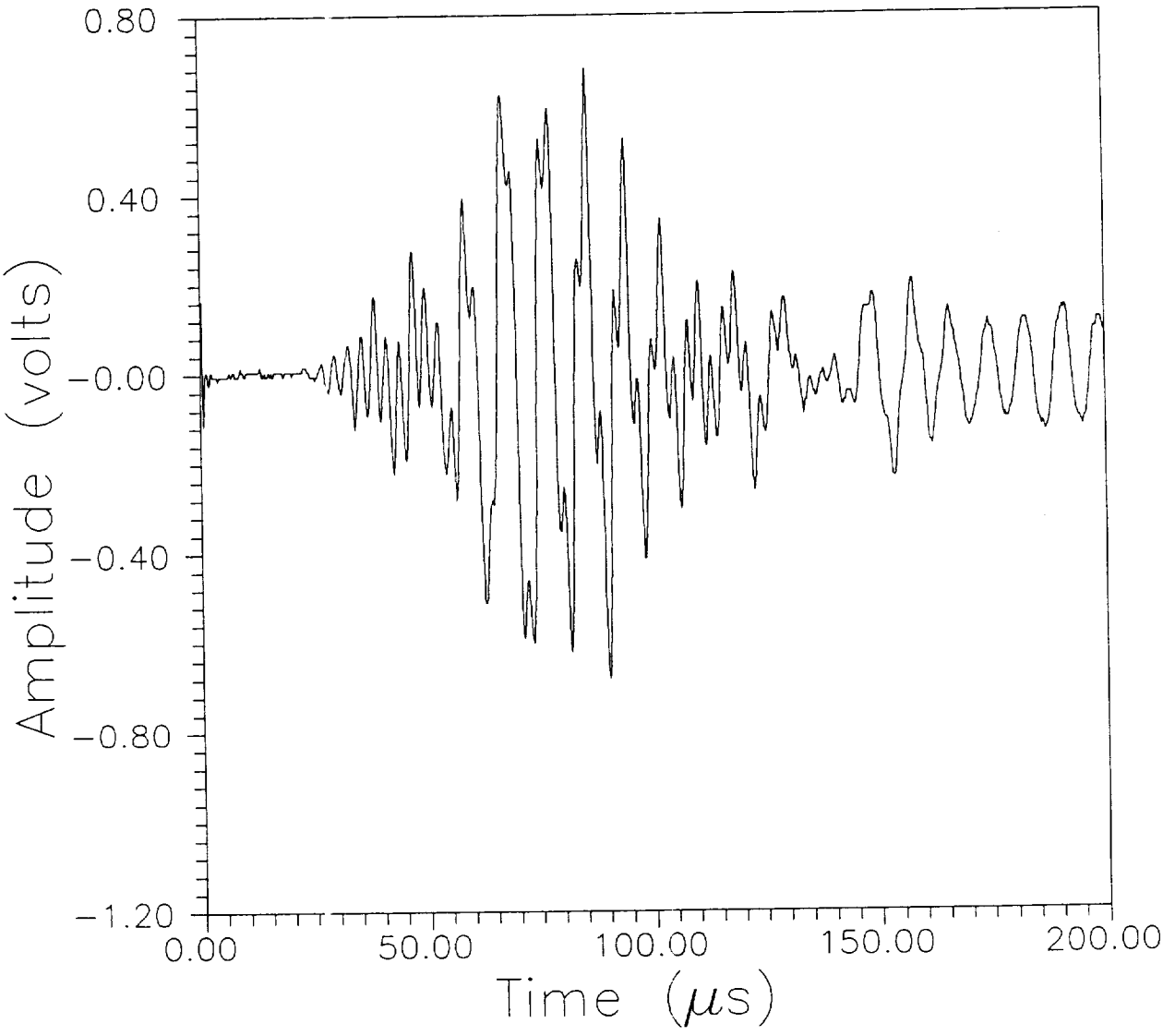

Figure 33. AET 206 AU unit detected waveform for the graphite/epoxy 90 degree laminate specimen.

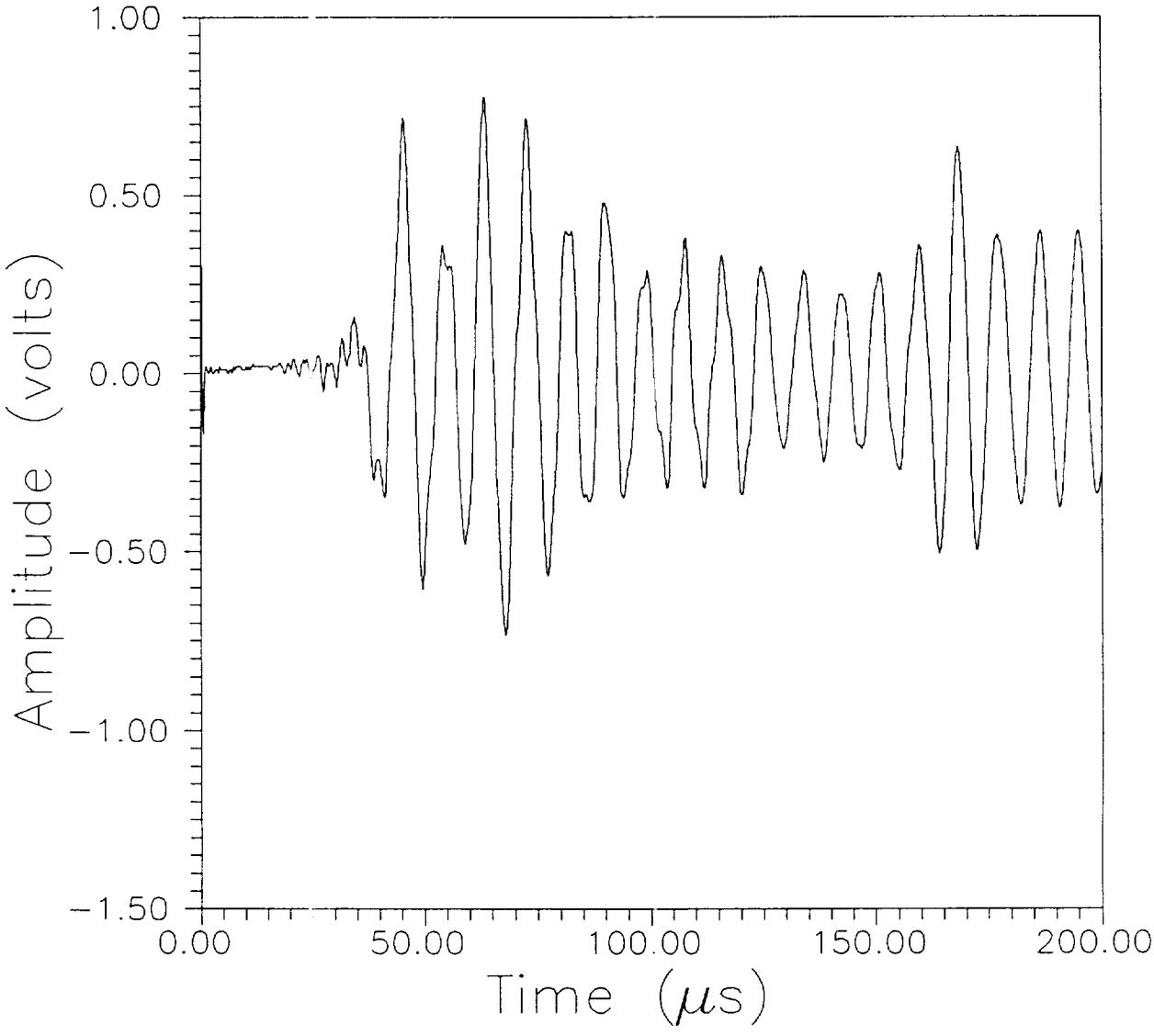

Figure 34. AET 206 AU unit detected waveform for the graphite/epoxy cross-ply laminate specimen.

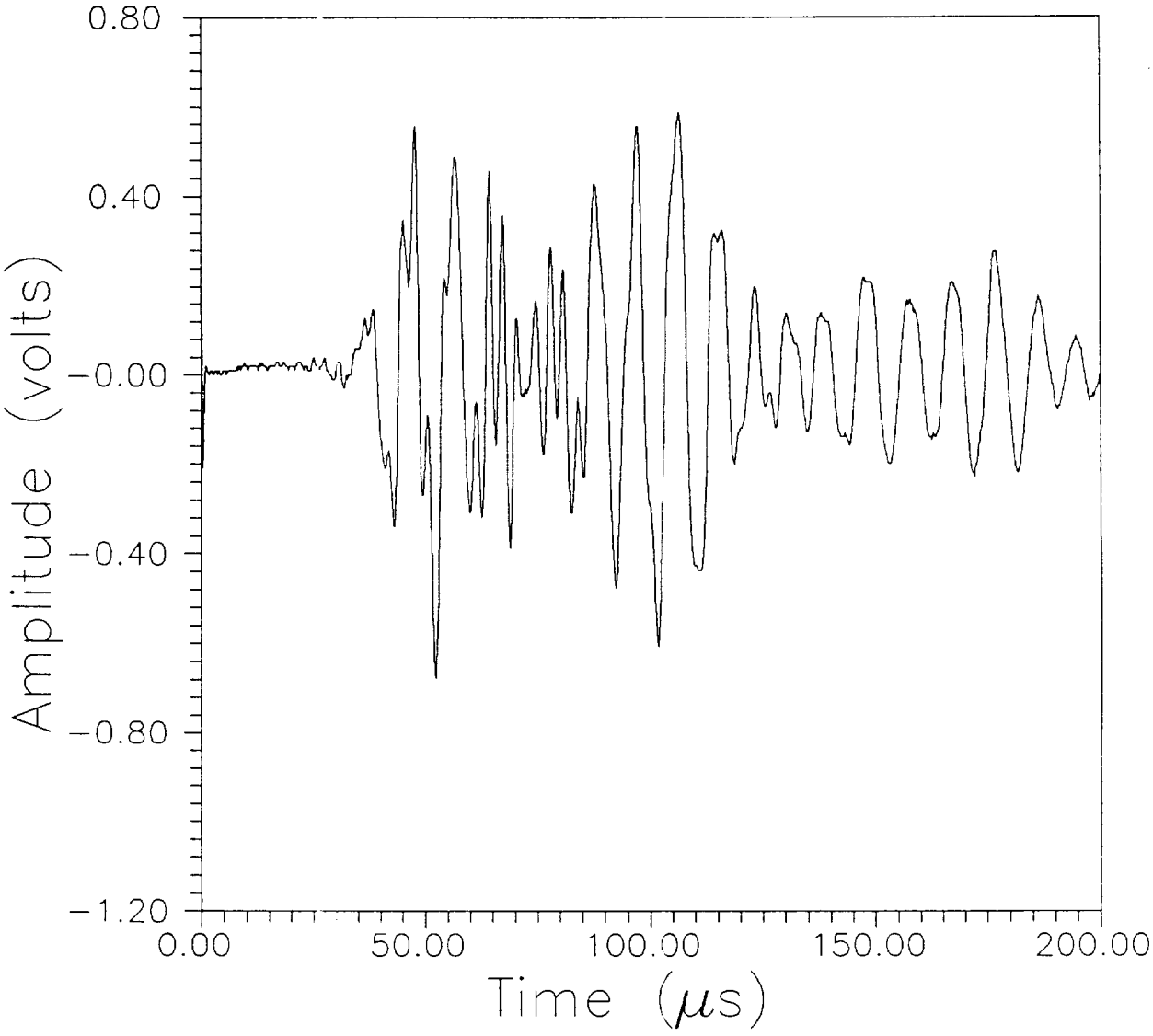

Figure 35. AET 206 AU unit detected waveform for the filament wound composite specimen.

CONCLUSIONS

This research has shown that replacement of conventional piezoelectric transducers with a laser generation/detection system permitted true non-contact acousto-ultrasonic measurements to be made. The fiber-optic heterodyne interferometer used in this system captured waveforms which corresponded extremely well with theoretical predictions, while conventional piezoelectric transducers did not. Among the waveforms faithfully recorded were an acoustic emission signal from breaking a glass capillary, 5 MHz piezoelectric transducer generated ultrasound propagating through an aluminum block, pulsed laser generated waves in a brass plate and an aluminum block, and acousto-ultrasonic waveforms from graphite/epoxy laminates and a filament wound composite. A state-of-the-art laser based acousto-ultrasonic system, incorporating a compact pulsed laser and a fiber-optic heterodyne interferometer, was delivered to the NASA Lewis Research Center along with this final report.

For the acousto-ultrasonic technique, the effects of piezoelectric transducer ringing are eliminated using the laser based system, which leads to a stress-wave-factor which is a measure of the wave propagating through the test material only and thus faithfully characterizes the material. The added benefit of being able to use this and other laser ultrasonic systems in hostile and unusual environments such as outer space makes them worthy of consideration for many future nondestructive evaluation applications.

REFERENCES

1. R.E. Green, Jr., Ultrasonic Investigation of Mechanical Properties, Vol. III, Treatise on Materials Science and Technology, Academic Press, New York (1973).

2. R.E. Green, Jr., Effect of Metallic Microstructure on Ultrasonic Attenuation, in Nondestructive Evaluation: Microstructural Characterization and Reliability Strategies, O. Buck and S.M. Wolf (eds.), The Metallurgical Society of AIME, Warrendale, PA, (1981) pp.115-132.

3. R.M. White, Generation of Elastic Waves by Transient Surface Heating, J. Appl. Phys. 34, 3559-3567 (1963).

4. A.N. Bondarenko, Yu.B. Drobat and S.V. Kruglov, Optical Excitation and Detection of Nanosecond Acoustic Pulses in Nondestructive Testing, Soviet J. NDT 12, 655-658 (1976).

5. H.M. Ledbetter and J.C. Moulder, Laser-Induced Rayleigh Waves in Aluminum, J. Acoust. Soc. Amer. 65, 840-842 (1979).

6. C.A. Calder and W.W. Wilcox, Non-Contact Material Testing Using Laser Energy Deposition and Interferometry, Mater. Eval. 38, 86-91 (1980).

7. R.L. Wellman, Laser System for the Detection of Flaws in Solids, Harry Diamond Laboratories, Report No. HDL-TR-1902 (1980).

8. R.J. Dewhurst, A Hand-Held Laser-Generator of Ultrasonic Pulses, NDT Communications 1, 93-103 (1983).

9. M.J. Rudd and J.A. Doughty, Laser Generation of Ultra sound, Naval Air Development Center, Report No. NADC-81067-60 (1983).

10. A.M. Aindow, R.J. Dewhurst, S.B. Palmer, and C.B. Scruby, Laser-Based Non-Destructive Testing Techniques for the Ultrasonic Characterization of Subsurface Flaws, NDT International 17, 329-335 (1984).

11. E. Bourkoff and C.H. Palmer, Low-Energy Optical Generation and

Detection of Acoustic Pulses in Metals and Nonmetals, Appl. Phys. Lett. 46, 143-145 (1985).

12. W.R. Prosser and R.E. Green, NDE of Composites Using Laser Generated Acoustic Waves, Proceedings of the 1985 Spring Conference of the Society for Experimental Mechanics, Las Vegas, NV(June 1985)

13. D.A. Hutchins, "Ultrasonic Generation by Pulsed Lasers", Physical Acoustics, Vol. XVIII, pp. 21-123 (1988).

14. J.-D. Aussel and J.-P. Monchalin, "Measurement of Ultrasound Attenuation by Laser Ultrasonics", J. Appl. Phys. 65, - (1989)

15. A.D.W. McKie, J.W. Wagner, J.B. Spicer and J.B. Deaton, Jr., "Narrowing the Bandwidth of Generated Ultrasound by Laser Illumination of Aluminum with an Array Source", Ultrasonics International '89 (Madrid, Spain) to be published by Butterworths, London (1990).

16. J.W. Wagner, A.D.W. McKie, J.B. Spicer and J.B. Deaton, Jr., "Laser Generation of Directed Ultrasound in Solids Using Spatial and Temporal Beam Modulation", Review of Progress in Quantitative NDE, Vol. 9 (Brunswick, Maine) (1990).

17. C.H. Palmer and R.E. Green, Jr., Optical Detection of Acoustic Emission Waves, Appl. Opt. 16, 2333-2334 (1977).

18. R.A. Kline, R.E. Green, Jr., and C.H. Palmer, A Comparison of Optically and Piezoelectrically Sensed Acoustic Emission Signals, J. Acoust. Soc. Amer. 64, 1633-1639 (1978).

19. C.H. Palmer and R.E. Green, Jr., Optical Probing of Acoustic Emission Waves, in Nondestructive Evaluation of Materials, J.J. Burke and V. Weiss (eds.), Plenum Publishing, New York (1979) pp.347-378.

20. J.T. Glass and R.E. Green, Jr., Acoustic Emission During Deformation and Fracture of Three Naval Alloy Steels, Materials Evaluation 43, 864-872 (1985).

21. J.-P. Monchalin, "Optical Detection of Ultrasound", IEEE Transactions on Ultrasonics, Ferroelectrics, and Frequency Control, Vol. UFFC-33 (1986).

22. J.W. Wagner, "Optical Detection of Ultrasound", Physical Acoustics, Vol. XIX (to be published)

23. G.A. Matzkanin, G.L. Burkhardt, and C.M. Teller, Nondestructive Evaluation of Fiber Reinforced Epoxy Composites: A State of the Art Survey, AD AO71-973, April 1979, 198 pages.

24. M.J. Golis, R.P. Mester, J.L. Crowe, and G.J. Posakony, Investigation of Techniques to Nondestructively Test Reinforced Plastic Composite Pipe. AD 744 294, December 1973, 148 pages.

25. C.N. Owston, Carbon Fiber Reinforced Polymers and Nondestructive Testing, British Journal of NDT, 15, 2-11 (1973).

26. R.M. Collins, NDT Chronology of Advanced Composites at Grumman Aerospace, Materials Evaluation 39, 1126-1129 (1981).

27. J.L. Cook, W.W. Reinhardt, and J.E. Zimmer, Development of Non-Destructive Test Techniques for Multidirectional Fiber Reinforced Resin Matrix Composites, AD 746 592, October 1971, 186 pages.

28. D.J. Hagemaier and R.H. Fassbender, Nondestructive Testing of Advanced Composites, Materials Evaluation, pp.43-49, (June 1979).

29. D.J. Hagemaier and R.H. Fassbender, Nondestructive Testing of Advanced Composites, Douglas Aircraft Paper 6774, presented at SAE Aerospace Meeting, pp.1-9, (Novermber 1978).

30. D. Hagemaier, H.J. McFaul, and D. Moon, Nondestructive Testing of Graphite Fiber Composite Structures, Materials Evaluation 29, 133-142.

31. E.G. Henneke and J.C. Duke, A Review of the State-of-the-Art of Nondestructive Evaluation of Advanced Composite Materials, Virginia Polytechnic Institute and State University, Department of Engineering Science and Mechanics, Blacksburg, VA (September 1979).

32. D.H. Kaelble, Quality Control and Nondestructive Evaluation Techniques for Composites - Part I: Overview of Characterization Techniques for Composite Reliability,
AD A118 410, (May 1982), 79 pages.

33. J.P. Maigret and G. Jube, Advanced NDT Methods for Filament Wound Pressure Vessels and Composites in General, SAMPE, Science of Advanced Materials and Process Engineering Series, 16, 123-137 (1971).

34. George A. Matzkanin, Nondestructive Evaluation of Fiber Reinforced Composites, A State-of-the-Art Survey, Vol.1, NDE of Graphite Fiber Reinforced Plastic Composites, NTIAC 82-1, March 1982, 62 pages.

35. Sharon A. McGovern, NDI Survey of Composite Structures, AD A081801, January 1980, 66 pages.

36. R.B. Pipes (ed.), Nondestructive Evaluation and Flaw Criticality for Composite Materials, ASTM STP 696, October 1978.

37. R. Prakash, Nondestructive Testing of Composites, Composites 11, 217-224 (1980).

38. W.N. Reynolds, Nondestructive Examination of Composite Materials, A Survey of European Literature, AD A100454, AVRADCOM Report No. TR 81-F-6, May 1981, 76 pages.

39. I.G. Scott and C.M. Scala, NDI of Composite Materials, AD A106278, July 1981, 30 pages.

40. Alex Vary, A Review of Issues and Strategies in Nondestructive Evaluation of Fiber Reinforced Structural Composites, 11th National SAMPE Technical Conference, Materials and Processes for the Eighties, November 1979, pp. 166-177.

41. Nondestructive Testing, A Survey, NASA SP 5113, 1973, 282 pages.

42. R.A. Blake, Jr., Ultrasonic NDE of Composite Materials, Center for Composite Materials Report CCM-79-3, The University of Delaware, Newark, December 1979, 114 pages.

43. Albert M. Lindrose, Ultrasonic Wave and Moduli Changes in a Curing Epoxy Resin, Experimental Mechanics, 18, 227-232 (1978).

44. E.G. Henneke, W.W. Stinchcomb, and K.L. Reifsnider, Some Ultrasonic Methods for Characterizing Response of Composite Materials, NBS Special Publication 596, Ultrasonic Materials Characterization.

45. W. Hand, M. Silvergleit, and G.R. Arcus, Nondestructive Ultrasonic Examination of Epoxy Glass Reinforced, Filament Wound, Cylindrical Deep Submergence Test Models, Report 9-32 DTNSRDC, October 1970, 49 pages.

46. B.R. Jones and D.E.W. Stone, Towards an Ultrasonic-Attenuation Technique to Measure Void Content in Carbon Fibre Composites, Nondestructive Testing 9, 71-79 (1976).

47. B.G. Martin, Ultrasonic Attenuation Due to Voids in Fiber Reinforced Plastics, NDT International 9, 242-246 (1976).

48. D.E.W. Stone, Non-Destructive Inspection of Composite Material for Aircraft Structural Applications, British Journal of NDT, March 1978, pp.65-75.

49. D.E.W. Stone and B. Clark, Ultrasonic Attenuation as a Measure of Void Content in Carbon Fibre Reinforced Plastics, Non-Destructive Testing 8, 137-145 (1975).

50. W.H.M. Van Dreumel, Ultrasonic Scanning for Quality Control of Advanced Composites, NDT International 11, 233-235 (1978).

51. D.S. Forli and S. Torp, NDT of Glass Fiber Reinforced Plastics (GRP), Paper 4B2 Eighth World Conference on NDT, Cannes, France (1976).

52. R. Prakash and C.N. Owston, Ultrasonic Determination of Lay-up Order in Cross Plied CFRP, Composites 8, 100-102 (1977).

53. J.H. Williams and B. Dole, Ultrasonic Attenuation as an Indicator of Fatigue Life of Graphite/Epoxy Fiber Composites, NASA Contractor Report 3179, December 1179, 19 pages.

54. M. Meron, Y. Bar-Cohen, and O. Ishai, Nondestructive Evaluation of Strength Degradation in Glass-Reinforced Plastic as a Result of

Environmental Effects, Journal of Testing and Evaluation, 5, 394-396 (1977).

55. Alex Vary, Quantitative Ultrasonic Evaluation of Engineering Properties in Metal, Composites and Ceramics, NASA-TM-81530, 1980, 18 pages.

56. A. Vary and K.J. Bowles, An Ultrasonic-Acoustic Technique for Nondestructive Evaluation of Fiber Composite Quality, Polymer Engineering and Science, 9, 373-376 (1979).

57. A. Vary and K.J. Bowles, Ultrasonic Evaluation on the Strength of Unidirectional Graphite/Polymide Composites, 11th Symposium on Nondestructive Evaluation, April 1977, San Antonio, TX, 26 pages.

58. A. Vary and R.F. Lark, Correlation of Fiber Composite Tensile Strength with the Ultrasonic Stress Wave Factor, Journal of Testing and Evaluation 7, 185-191 (1979).

59. Y. Bar-Cohen, E. Harnik, M. Meron, and R. Davidson, Ultrasonic Nondestructive Evaluation Method for the Detection and Identification of Defects in Filament Wound Glass Fiber-Reinforced Plastic Tubes, Materials Evaluation 37, 51-55 (1979).

60. G.P. Capsimalis, G. D'Andrea, and R. Peterson, Ultrasonic and Acoustic Holographic Techniques for Inspection of Composite Gun Tubes and Other Weapon Components, AD-A039 605, March 1977, 57 pages.

61. Y. Bar-Cohen, U. Arnon, and M. Meron, Defect Detection and Characterization in Composite Sandwich Structure by Ultrasonics, SAMPE Journal 14, 4-8 (1978).

62. T. Liber, I.M. Danier, and S.W. Schramm, Ultrasonic Techniques for Inspecting Flat and Cylindrical Composite Specimens, ASTM STP 696, Nondestructive Evaluation and Flaw Criticality for Composite Structures, R.B. Pipes (Ed.),
pp. 5-25, (1978).

63. S. Friedman and M. Silvergleit, The Nondestructive Evaluation of Graphite/Epoxy Composite Materials, DTNSRDC Center Report TM-28-75-248, April 1976.

64. Y. Bar-Cohen, M. Meron, and O. Ishai, Nondestructive Evaluation of Hygrothermal Effects on Fiber-Reinforced Plastic Laminates, Journal of Testing and Evaluation 7, 291-296 (1979).

65. A. Vary, The Feasibility of Ranking Material Fracture Toughness by Ultrasonic Attenuation Measurements, NASA Technical Memorandum NASA TM X-71769 (1975).

66. A. Vary, The Feasibility of Ranking Material Fracture Toughness by Ultrasonic Attenuation Measurements, J. of Testing and Evaluation 4, 251-256 (1976)

67. A. Vary and K.J. Bowles, Ultrasonic Evaluation of the Strength of Unidirectional Graphite-Polyimide Composites, NASA TM-X-73646 (1977).

68. A. Vary and K.J. Bowles, Use of an Ultrasonic-Acoustic Technique for Nondestructive Evaluation of Fiber Composite Strength, NASA TM-73813 (1978).

69. A. Vary and K.J. Bowles, An Ultrasonic-Acoustic Technique for Nondestructive Evaluation of Fiber Composite Quality, Polymer Engr. & Sci. 19, 373-376 (1979).

70. A. Vary and R.F. Lark, Correlation of Fiber Composite Tensile Strength with the Ultrasonic Stress Wave Factor, NASA TM-78846 (1978).

71. A. Vary and R.F. Lark, Correlation of Fiber Composite Tensile Strength with the Ultrasonic Stress Wave Factor, J. of Testing and Evaluation 7, 185-191 (1979).

72. A. Vary, Correlations Among Ultrasonic Propagation Factors and Fracture Toughness Properties of Metallic Materials, NASA Technical Memorandum NASA TM X-71889 (1976).

73. A. Vary, Correlations Among Ultrasonic Propagation Factors and Fracture Toughness Properties of Metallic Materials, Materials Evaluation 36, 55-64 (1978).

74. A. Vary, Quantitative Ultrasonic Evaluation of Mechanical Properties of Engineering Materials, NASA Technical Memorandum NASA TM-78905 (1978).

75. A. Vary, Correlations Between Ultrasonic and Fracture Toughness Factors in Metallic Materials, STP 677, American Society for Testing and Materials, Philadelphia, PA (1979) pp. 563-578.

76. A. Vary, Ultrasonic Measurement of Material Properties, in Research Techniques in Nondestructive Testing, Vol. IV, R.S. Sharpe (ed.), Academic Press, NY (1980) pp.159-204.

77. A. Vary, Concepts and Techniques for Ultrasonic Evaluation of Material Mechanical Properties, in Mechanics of Nondestructive Testing, W.W. Stinchcomb (ed.), Plenum Press, NY (1980) pp.123-141.

78. A. Vary and D.R. Hull, Interrelation of Material Microstructure, Ultrasonic Factors, and Fracture Toughness of a Two Phase Titanium Alloy, NASA Technical Memorandum 82810 (1982).

79. A. Vary, Fundamentals of Ultrasonic NDE for Microstructure/Material Property Interrelations, Reprint from CP-2251, Advanced Materials Technology Seminar held at NASA Langley Research Center, Hampton, VA (November 1982).

80. A. Govada and J.C. Duke, Jr., "Application of Ultrasonics to Damage Development in Metal Matrix Composites", ASNT Paper Summaries, (1982), pp. 379-385.

81. Duke, J.C., Jr., Henneke, E.G., II, Stinchcomb, W.W., and Reifsnider, K.L., "Characterization of Composite Materials by Means of the Ultrasonic Stress Wave Factor", in Composite Structures 2, I.H. Marshall (Ed.), Applied Scientific Publishers, (1983), pp. 53-60.

82. Govada, A.K., Duke, J.C., Jr., Henneke, E.G., II and Stinchcomb, W.W., "A Study of the Stress Wave Factor Technique for the Characterization of Composite Materials", Center for Composite Materials and Structures Report CCMS 84-13, Virginia Polytechnic Institute and State University, Blacksburg, VA (1984).

83. Vary, A., "Ultrasonic Nondestructive Evaluation, Microstructure, and Mechanical Property Interrelations", NASA Technical Memorandum 86876 (1984).

84. Vary, A., (ed.), Proceedings of Analytical Ultrasonics

in Materials Research and Testing Conference, NASA Lewis Research Center, Cleveland, OH (1984).

85. Henneke, E.G. II, Duke, J.C. Jr., Stinchcomb, W.W., Govada, A. and Lemascon, A., "A Study of the Stress Wave Factor Technique for the Characterization of Composite Materials", NASA CR 3670.

86. Govada, A.K.; Duke, J.C.; Henneke II, E.G.; Stinchcomb, W.W., "A Study of the Stress Wave Factor Technique for the Characterization of Composite Materials", NASA Contractor Report 174870, February 1985.

87. Sarrafzadeh-Khoee, A.; Kiernan, M.T.; Duke, Jr., J.C.; Henneke II, E.G., "A Study of the Stress Wave Factor Technique for Nondestructive Evaluation of Composite Materials", NASA Contractor Report 4002, July 1986.

88. Duke, Jr., J.C.; Henneke II, E.G.; Kiernan, M.T.; Grosskopf, P.P., "A Study of the Stress Wave Factor Technique for Evaluation of Composite Materials", NASA Contractor Report 4195, January 1989.

89. Dos Reis, H.L.M., and McFarland, D.M., "On The Acousto-Ultrasonic Characterization of Wood Fiber Hardboard", J. of Acoustic Emission, Vol. 5 Number 2, (1986) pp. 67-70.

90. Dos Reis, H.L.M., "Acousto-Ultrasonics:Applications to Wire Rope, Wood Fiber Hardboard, and Adhesion", Acousto Ultrasonics: Theory and Application, ed. J.C. Duke Jr., Plenum Press, New York, 1988.

91. Patton-Mallory, M., and Anderson, K.D., "An Acousto-Ultrasonic Method for Evaluating Wood Products", Acousto-Ultrasonics: Theory and Application, ed. J.C. Duke Jr., Plenum Press, New York, 1988.

92. Mittelmal, A., Roman, I., Bivas, A., Leichter, I., Margulies, J.Y., and Weinreb, A., "Acousto-Ultrasonic Characterization of Physical Properties of Human Bones", Acousto-Ultrasonics: Theory and Application, ed. J.C. Duke Jr., Plenum Press, New York, 1988.

93. Williams, J.H. Jr., Hainsworth, J., and Lee, S.S., "Acoustic-Ultrasonic Nondestructive Evaluation of Double-Braided Nylon Ropes Using the Stress Wave Factor", Fibre Science and Technology, 21 1984, pp.169-180.

94. De, A., Phani, K.K., and Kumar, S., "Acousto-Ultrasonic Study on Glass-Ceramics in the System MgO-Al2O3-SiO2, J of Materials Science Letters 6 1987, pp. 17-19.

95. Williams, J.H., Lee, S.S., and Wang, T.K., "Nondestructive Evaluation of Strength and Separation Modes in Adhesively Bonded Automotive Glass Fiber Composite Single Lap Joints", J. of Composite Materials, Vol. 21 1987, pp.14-35.

96. Srivastava, V.K., and Prakash, R., "Acousto-Ultrasonic Evaluation of the Strength of Composite Material Adhesive Joints", Acousto-Ultrasonics: Theory and Application, ed. J.C. Duke Jr., Plenum Press, New York, 1988.

97. Tanary, S., "Characterization of Adhesively Bonded Joints Using Acousto-Ultrasonics" Masters Essay, University of Ottawa, 1988.

98. Russell-Floyd, R.; Phillips, M.G., "A Critical Assessment of Acousto-Ultrasonics as a Method of Nondestructive examination for Carbon-Fibre-Reinforced Thermoplastic Laminates", NDT International, August (1988) pp.247-257.

99. Bhatt, M.; Hogg, P.J., "Test Conditions in Stress Wave Factor Measurements for Fibre-Reinforced Composites and Laminates", NDT International, February 1988, pp. 3-10.

100. Phani, K.K., and Bose, N.R., "Hydrothermal Aging of Csm-Laminate During Water Immersion - An Acousto-Ultrasonic Study", J. of Materials Science, (21) 1986, pp.3633-3637.

101. Phani, K.K., and Bose, N.R., "Hydrothermal Aging of Jute-Glass Fiber Hybrid Composites - An Acousto-Ultrasonic Study", J. of Materials Science, (22) 1987 pp.1929-1933.

102. Talreja, R., Govada, A., and Henneke, E.G.II, "Quantitative Assessment of Damage Growth in Graphite/Epoxy Lamiates by Acousto-Ultrasonic Measurements", Review of Progress in Qunatitative Nondestructive Evaluation, Vol 3B, ed. D.O. Thompson and D.E. Chimenti, Plenum Press, New York, 1984, pp.1099-1106.

103. Williams, J.H. Jr., and Lampert, N.R., "Ultrasonic Evaluation of Impact-Damaged Graphite Fiber Composites", Materials Evaluation, Vol 38., No. 12, 1980, pp.68-72.

104. Talreja, R., "Application of Acousto-Ultrasonics to Quality Control and Damage Assessment of Composites", Acousto-Ultrasonics: Theory and Application, ed. J.C. Duke Jr., Plenum Press, New York, 1988.

105. Mitchell, J.R., "Multi-Parameter, Multi-Frequency Acousto-Ultrasonic for Detecting Impact Damage in Composites", Acousto-Ultrasonics: Theory and Application, ed. J.C. Duke Jr., Plenum Press, New York, 1988.

106. Duke, J.C. Jr., and Kiernan, M.T., "Predicting Damage Development in Composite Materials Based on Acousto-Ultrasonic Evaluation", Acousto-Ultrasonics: Theory and Application, ed. J.C. Duke Jr., Plenum Press, New York, 1988.

107. Hemann, J.H., Cavano, P., Kautz, H., and Bowles, K., "Trans-Ply Crack Density Detection by Acousto-Ultrasonics", Acousto-Ultrasonics: Theory and Application, ed. J.C. Duke Jr., Plenum Press, New York, 1988.

108. Phani, K.K., Niyogi, S.K., Maitra, A.K., Roychaudhury, M., "Strength and Elastic Modulus of a Porous Brittle Solid: An Acousto-Ultrasonic Study", J. of Materials Science, (21) 1986 pp.4335-4341.

109. Dos Reis, H.L.M., and Kautz, H.E., "Nondestructive Evaluation of Adhesive Bond Strength Using the Stress Wave Factor Technique", J. of Acoustic Emission, Vol. 5 No. 4, 1986 pp. 144-147.

110. Brahma, K.K., and Murthy, C.R.L., "Bond Quality Evaluation of Bimetallic Strips: Acousto-Ultrasonic Approach", Acousto-Ultrasonics: Theory and Application, ed. J.C. Duke Jr., Plenum Press, New York, 1988.

111. Kiernan, M.T., Duke, Jr., J.C., "Acousto-Ultrasonics as a Monitor of Material Anisotropy", Materials Evaluation, Vol. 46, July 1988 pp.1105-1113.

112. Kautz, Harold E., "Acousto-Ultrasonic Verification of the Strength of Filament Wound Composite Material", NASA Technical Memorandum 88827, July 21-24, 1986.

113. Kautz, Harold E., "New Acousto-Ultrasonic Techniques Applied to Aerospace Materials", NASA Technical Memorandum 101299, August 9-12, 1988.

114. Sarrafzadeh-Khoee, A., and Duke, Jr., John C., "Noncontacting Detection in Ultrasonic NDE of Materials: Simple Optical Sensor and Fiber Optics Interferometric Application" found in"Ultrasonic Stress Wave Characterization of Composite Materials", NASA Contractor Report 3976, May 1986.

115. Sarrafzadeh-Khoee, A., Kiernan, M.T., Duke, J.C., Jr., and Henneke, E.G., II, "A Study of the Stress Wave Factor Technique for Nondestructive Evaluation of Composite Materials", NASA Contractor Report 4002, July 1986.

116. Duke, J.C., Jr., Henneke, E.G., II, Kiernan, M.T., and Grosskopf, P.P., "A study of the Stress Wave Factor Technique for Evaluation of Composite Materials", NASA Contractor Report 4195, January 1989.

117. Wagner, J.W., "Optical Generation and Detection of Ultrasound for Flaw Detection and In-Line Process/Quality Control", Proceedings of the ASM Metals Congress, Detroit, MI (Sept. 1984), American Society for Metals, Metals Park, OH (1985).

118. Wagner, J.W. and Spicer, J.B., "Intrinsic Sensitivity Limitations in Classical Interferometers," in Nondestructive Characterization of Materials II, J.F. Bussiere et al. (Eds.), PLenum Press, N.Y., pp.761-770 (1987).

119. Wagner, J.W. and Green, R.E., Jr.,"Optical Generation and Detection of Ultrasound", International Advances in NDE, Proceedings of the Conference on Nondestructive Evaluation for Aerospace Requirements, Huntsville, AL (August, 1987).

120. Wagner, J.W. and Spicer, J.B., "Theoretical Noise-Limited Sensitivity of Classical Interferometry", J. Optical Society of America, 4, 1316-1326 (1987).

121. Spicer, J.B. and Wagner, J.W., "Absolute Calibration of Interferometric Systems for Detection and Measurement of Surface Acoustic Waves", Applied Optics, 27, 3561-3566 (1988).

122. McKie, A.D.W. and Wagner, J.W., "Optical Sensing of IN-Plane Ultrasonic Transients", Appl. Phys. Lett. 53, 1043-1044 (1988).

123. Wagner, J.W., Deaton, J.B., Jr., and Spicer, J.B., "Generation of Ultrasound by Repetitively Q-Switching a Pulsed Nd:YAG Laser, Applied Optics 27, 4696-4700 (1988).

124. Wagner, J.W., Green, R.E., Jr., and Ehrlich, M.J., "Combined Optical and Acoustic Methods for Inspection of Composite Materials", in Materials Processes: The Intercept Point, Proceedings of the 20th International SAMPE Technical Conference, Minneapolis, MN, Vol. 20, pp. 490-504 (1988).

125. Wagner, J.W., and Deaton, J.B., "Laser Generation of Narrow Band Ultrasound", 1988 Review of Progress in Quantitative NDE, La Jolla, CA, Vol. 8A, pp. 505-512 (1989).

126. Wagner, J.W., "Optical Detection of Ultrasonic Disturbances", J. Laser Applications 1, 59-64 (1989).

127. Spicer, J.B. and Wagner, J.W., "Fiber-Optic Based Interferometer for Noncontact Ultrasonic Determination of Acoustic Velocity and Attenuation in Materials", in Nondestructive Characterization of Materials, P. Holler et al. (Eds.), Springer-Verlag, N.Y., pp. 691-698 (1989).

128. McKie, A.D.W., Wagner, J.W., Spicer, J.B., and Penney, C.M., "Laser Generation of Narrowband and Directed Ultrasound", Ultrasonics 27, 323-330 (1989).

129. Glass, J.T.; Majerowicz, S.; Green, Jr., Robert E., "Acoustic Emission Determination of Deformation Mechanisms Leading to Failure of Naval Alloys", David Taylor Naval Ship R&D Center: Report No. DTNSRDC SME-CR-18-83, Vol. II, May 1983.

130. Hsu, N.N., "Dynamic Green's Functions of an Infinite Plate- A Computer Program", U.S. Department of Commerce, National Bureau of Standards, Report #NBSIR 85-3234, 1985.